INTERNATIONAL ATOMIC ENERGY AGENCY
UNITED NATIONS EDUCATIONAL, SCIENTIFIC AND CULTURAL ORGANIZATION

INTERNATIONAL CENTRE FOR THEORETICAL PHYSICS
34100 TRIESTE (ITALY) - P.O.B. 586 - MIRAMARE - STRADA COSTIERA 11 - TELEPHONE: 2240-1
CABLE: CENTRATOM - TELEX 460392-I

H4.SMR/381-43

COLLEGE ON ATOMIC AND MOLECULAR PHYSICS: PHOTON ASSISTED COLLISIONS IN ATOMS AND MOLECULES

(30 January - 24 February 1989)

EXPERIMENTAL ASPECTS OF LICET

M. MATERA

IEQ-CNR
Firenze, Italy

Lecture notes

EXPERIMENTAL ASPECTS OF LICET

Manlio Matera

Institute of Quantum Electronics
Via Panciatichi, 56/30
50127 Firenze, Italy

Summary :

1. The physical process

Collision-induced radiative transitions are represented by the reaction:

$$A_i + B_i + n\hbar\omega \longrightarrow A_f + B_f + (n \pm 1)\hbar\omega$$

where: $A_{i,f}$, $B_{i,f}$ are initial and final electronic states of atoms A and B respectively;

n is the number of photons of a laser field of frequency ω.

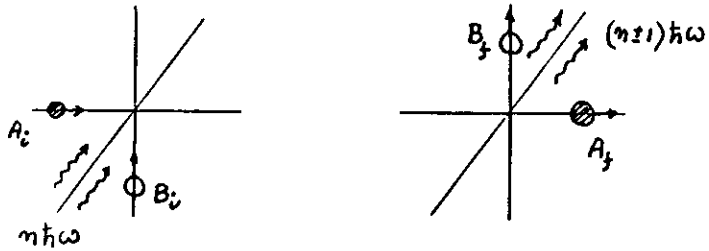

The process requires the simultaneous presence of a laser field and a collision and can take place in absorption or in emission.

If only one atom changes its state, while the other acts as a perturber:

$$A + B + \hbar\omega \longrightarrow A^* + B$$

the process is called CARE (Collisionally Assisted Radiative Excitation).

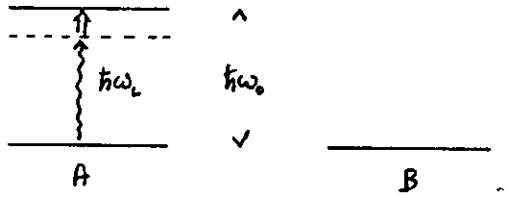

The collision is conveniently studied in the reference system where one atom is at rest:

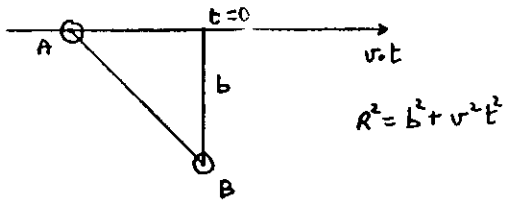

b = impact parameter

v = mean relative velocity

R = interatomic distance

Definition of <u>mean collision time</u>:

$$\tau = b/v$$

For a typical collision:

$b \approx 10$ Å $v \approx 10^5$ cm/sec

$t \approx 1$ psec

Definition of <u>detuning</u> of the laser from the resonance: $\Delta\omega = \omega_L - \omega_0$.

$|\Delta\omega| \ll \frac{1}{\tau}$ <u>Impact region</u>

The spectral profile in this region is Lorentzian, depending on the distribution of time between collisions;

$|\Delta\omega| \gg \frac{1}{\tau}$ { <u>Static region</u> / <u>Antistatic region</u>

Outside the impact region the spectral profile is strongly asymmetrical . In the static region it is determined by the

dynamics of the collision and, within the Born-Oppenheimer approximation, it can be related to adiabatic potential energy curves:

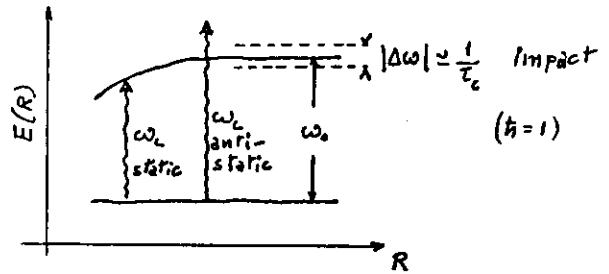

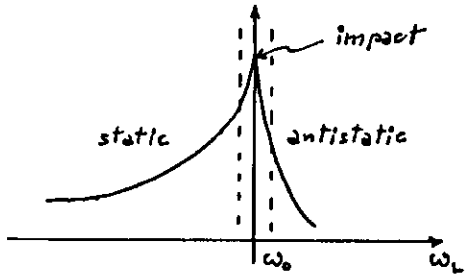

If both atoms undergo a transition:

$$A^* + B + \hbar\omega \longrightarrow A + B^{**}$$

the process is called LICET (Laser Induced Collisionally Energy Transfer).

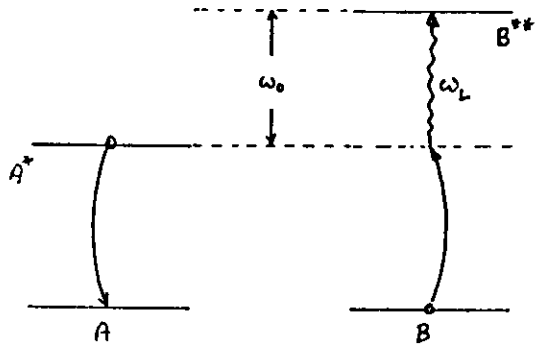

During a collision atom A transfers its excitation energy to atom B which, absorbing a photon, makes a transition to the highly-excited state B^{**}.

Even in this case the excitation spectrum (transition probability vs. laser frequency in the vicinity of ω_0) is asymmetrical, showing a marked wing on one side of ω_0 (static wing). The basic features of a LICET spectrum are explained in the framework of the atomic line broadening theory.

Collision-induced radiative transitions can be considered as a probe of collisional dynamics: by varying the frequency of the laser field it is possible to "select" collisions with small impact parameter, effective for the absorption of the photon.

The main goal of the study is the development of simple models describing accurately the collisional interaction of atoms in the presence of a laser field.

Perspective : study of laser assisted reactions between molecules (photochemistry).

Let us focus our attention on:

High resolution study of the spectral profile for the LICET process involving Europium and Strontium atoms.

The relevant energy levels are shown in figure 1, where $|\alpha_i\rangle$ and $|\beta_i\rangle$ label the atomic states in the absence of coupling (i.e. large interatomic distance).

The energy difference between states $|\alpha_1\rangle$ and $|\beta_2\rangle$: $\hbar\Delta = 63$ cm^{-1} is an important parameter for the interaction, called energy defect.

Initially the Eu atom is in the excited state $|\alpha_1\rangle$ and the Sr atom is in its ground state $|\beta_1\rangle$. During a collision the Eu atom

is deexcited, while the Sr atom is excited to the state $|\beta_2\rangle$, absorbing a photon from the laser field.

Experimentally the population of the final state is measured by monitoring the fluorescence emitted in the transition to the intermediate state $|\beta_2\rangle$.

2. Theoretical models

Even though many theoretical treatments of the LICET process have been published, we refer here to the model developed by A.Bambini and P.R.Berman, which has allowed to overcome some discrepancy between theory and experiment.

A convenient basis for the description of the system is provided by the compound states of the non interacting atoms:

$|i\rangle = |\alpha_i\rangle\,|\beta_i\rangle$ initial state

$|x\rangle = |\alpha_1\rangle\,|\beta_2\rangle$ intermediate state

$|f\rangle = |\alpha_1\rangle\,|\beta_3\rangle$ final state

The states $|i\rangle$ and $|x\rangle$ are coupled by the collisional interaction $\hat{V}_{AB}$, while the states $|x\rangle$ and $|f\rangle$ are coupled by the radiative interaction $\hat{W}_B$ of atom B. The Hamiltonian of the system can be therefore written:

$$\hat{H} = \hat{H}_0 + \hat{V}_{AB} + \hat{W}_B$$

where $\hat{H}_0$ is the Hamiltonian for the non-interacting atoms.

Assuming dipole-dipole interaction and neglecting the magnetic degeneracy of the atomic states we can write:

$$\hat{V}_{AB} \propto \frac{\hat{P}_A \hat{P}_B}{R^3}$$

where $\hat{P}_A$, $\hat{P}_B$ are the dipole moment operators and R is the interatomic distance.

For a classical laser field linearly polarized:

$$E = \frac{E_0}{2}\left(e^{i\omega_L t} + e^{-i\omega_L t}\right)$$

we have then: $$\hat{W}_B = \frac{\hat{P}_B E_0}{2}$$

The only nonvanishing matrix elements are:

$$\langle i|\hat{V}_{AB}|x\rangle = V_{ix}$$

$$\langle x|\hat{W}_B|f\rangle = \chi \quad \text{(Rabi frequency)}$$

Writing the eigenfunction in the form:

$$|\psi\rangle = a_i e^{-i\omega_i t}|i\rangle + a_x e^{-i\omega_x t}|x\rangle + a_f e^{-i\omega_f t}|f\rangle$$

the time-dependent Schrödinger equation:

$$i\frac{\partial}{\partial t}|\psi\rangle = \hat{H}|\psi\rangle$$

reduces to the system of differential equations:

$$\begin{cases} i\dot{a}_i = V_{ix}\, e^{i2\Delta t}\, a_x \\ i\dot{a}_x = V_{ix}\, e^{-i2\Delta t}\, a_i + \chi e^{-i(2\Delta+\Delta\omega)t}\, a_f \\ i\dot{a}_f = \chi\, e^{i(2\Delta+\Delta\omega)t}\, a_x \end{cases}$$

where $2\Delta = \omega_i - \omega_x$ energy defect

$\Delta\omega = \omega_L - (\omega_f - \omega_i)$ laser detuning

This system of equation can be solved numerically. However the statistics of the collisions (average over the impact parameters and over the interatomic velocities) makes approximate analytical solutions useful.

The main approximation used in most theoretical models are:

1 - classical and rectilinear atomic trajectories

2 - binary collisions

3 - long-range interaction potential (dipole-dipole)

4 - magnetic degeneracy of atomic states neglected.

The Bambini-Berman model has provided an analytical expression for the profile of the LICET spectrum in the static wing:

$$\sigma(\Delta\omega) \propto \frac{\chi^2}{(2\Delta + |\Delta\omega|)^{3/2} |\Delta\omega|^{1/2}}$$

This result was derived at first order in the laser field intensity, assuming the collisional interaction adiabatic.

Recent experimental studies have already provided a test of the model.

A prediction of the overall spectral shape can only be obtained by numerical calculations.

3. Experimental layout

The experimental apparatus used for LICET studies is shown in figure 2.

Two dye lasers, pumped by the same excimer laser, are used to pump the excited state $Eu(^8P_{9/2})$ and then to transfer the population to the final $Sr(^1D_2)$ state. The Europium and Strontium atoms are generated in a heat-pipe oven at a temperature T ≈ 750°C. The pulse of the transfer laser is delayed by 30 nsec in order to reduce direct two-photon absorption. The side-emitted fluorescence is focused onto the input slit of a monochromator, whose output is detected by a photomultiplier and measured by a gated integrator.

The control of the system and the data acquisition are made by a personal computer (figure 3). A drawing of the heat-pipe oven is shown in figure 4.

The configuration of the oscillators used for the dye lasers is shown in figure 5.

The main characteristics of the experimental apparatus required for an accurate measurement are the following:

- temporal stability of the dye lasers
- stability of the transfer laser emission versus frequency
- narrow bandwidth emission of the transfer laser
- high resolution, linearity and resettability of the frequency tuning of the transfer laser
- temporal stability of the atomic vapour densities
- low ASE (amplified stimulated emission) for the pump and transfer lasers.

The various parts of the apparatus have been optimized taking into account these requirements.

We discuss in the following the main background processes affecting the accuracy of the measurement.

1 - Direct two-photon absorption:

$$Sr\,(^1S_0) + \hbar\omega_1 + \hbar\omega_2 \longrightarrow Sr\,(^1D_2)$$

This process can produce a spurious peak on the LICET spectrum.

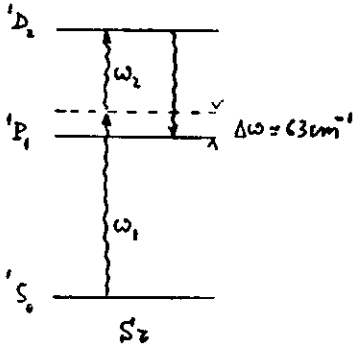

The effect can be minimized by:

- delaying the pulse of the transfer laser
- detuning the pump laser on the low frequency side of the transition $Eu(^8P_{9/2} - {}^8S_{7/2})$

2 - Direct two-step absorption of the wideband emission of the lasers:

$$Sr(^1S_0) + \hbar\omega_1 \longrightarrow Sr(^1P_1)$$

$$Sr(^1P_1) + \hbar\omega_2 \longrightarrow Sr(^1D_2)$$

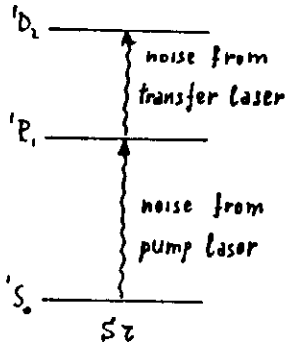

Typical emission spectrum of a dye laser:

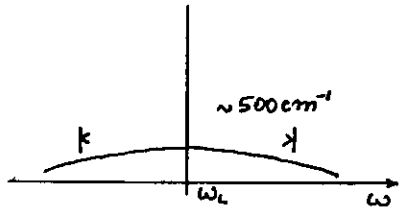

The effect, which is a background signal slowly dependent on the tuning frequency, can be reduced by optimizing the signal-to-noise ratio of the lasers. This has been accomplished using:

- a Moya cavity for the oscillator of the transfer laser
- a Strontium-vapour filter for the pump laser.

3 - Collision-induced two-step absorption (CARE)

$$Sr(^1S_0) + Ar + \hbar\omega_1 \longrightarrow Sr(^1P_1) + Ar$$

$$Sr(^1P_1) + Ar + \hbar\omega_2 \longrightarrow Sr(^1D_2) + Ar$$

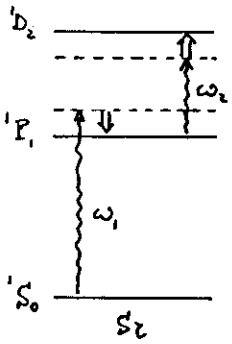

This effect, producing a background signal slowly dependent on frequency, can be reduced by lowering the buffer-gas density and using background subtraction techniques.

4 - Stimulated emission from the final level:

$$Sr(^1D_2) + n\hbar\omega \longrightarrow Sr(^1P_1) + (n+1)\hbar\omega$$

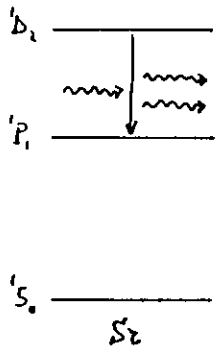

The stimulated emission can cause an anisotropy of the emitted

fluorescence dependent on the laser detuning and therefore affecting the LICET lineshape.

The effect can be minimized working at low densities or with a crossed beam geometry.

4. Results and discussion

Typical experimental conditions:

- vapour densities (at T ≈ 760 °C)

  N_{Eu} ≈ 10^{16} atoms/cm³

  N_{Sr} ≈ 10^{18} atoms/cm³

- energy/pulse

  pump laser E ≈ 50 μJ

  transfer laser E ≈ 0.3 mJ

- pulse duration

  T ≈ 30 nsec

- optical delay

  t ≈ 30 nsec

- emission bandwidth

  ≈ 0.1 cm^{-1}

- signal/noise ratio in the dye laser emission

  SNR < 5 x 10^{-3}

- resolution of the frequency tuning

  $\delta\omega$ < 0.1 cm^{-1}

A LICET spectrum measured over a detuning interval 100 ≈ cm^{-1} is shown in figure 6. The residual signal on the antistatic region is due to the background processes discussed above. The measurement has been done with higher frequency resolution in the core region (≈ 0.1 cm^{-1}) and lower in the static region (≈ 1.7 cm^{-1}). In a first analysis, the result of the measurement has been compared to the theoretical predictions separately, in the core and in the static wing.

Figure 7 shows a fit of the experimental data by the

Bambini-Berman analytical law. Figure 8 shows a comparison with the results of numerical calculations in the line-core, normalized to the peak value.

Finally the experimental data have been compared to the theory over all the spectrum, using a logarithmic compression of the frequency scale. In figure 9 :

- the continuous line represents the Bambini-Berman law;
- the circles represent numerical calculations normalized to the far wing behaviour.

From this analysis the following conclusions can be drawn:

1. the far-wing behaviour of the LICET spectrum is well described by the Bambini-Berman law;
2. there is a marked discrepancy between theory and experiment in the line core, showing that the measurement might have been affected by stimulated emission or some approximations used in the theoretical model may not be valid in this region of the line.

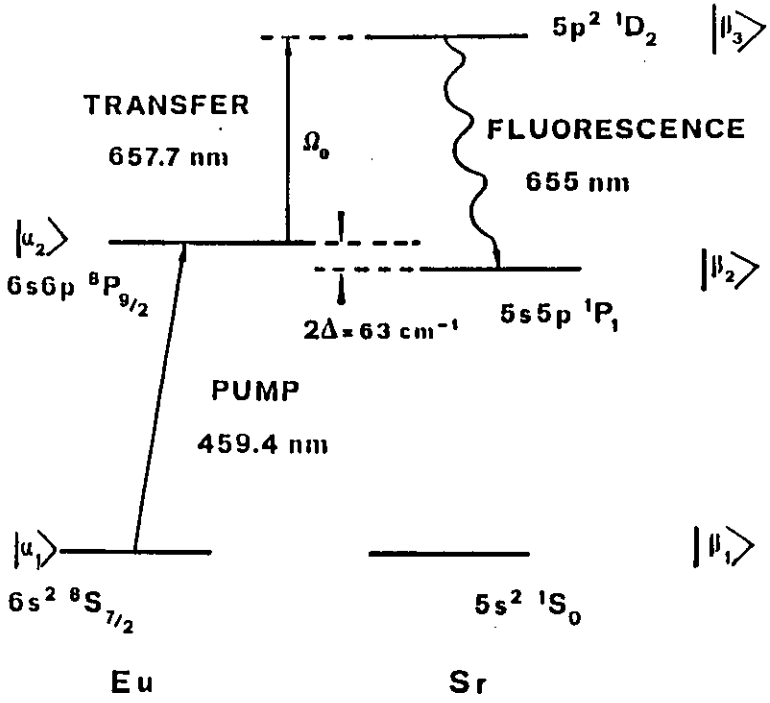

FIG. 1. Energy level diagram for the Eu-Sr laser induced process.

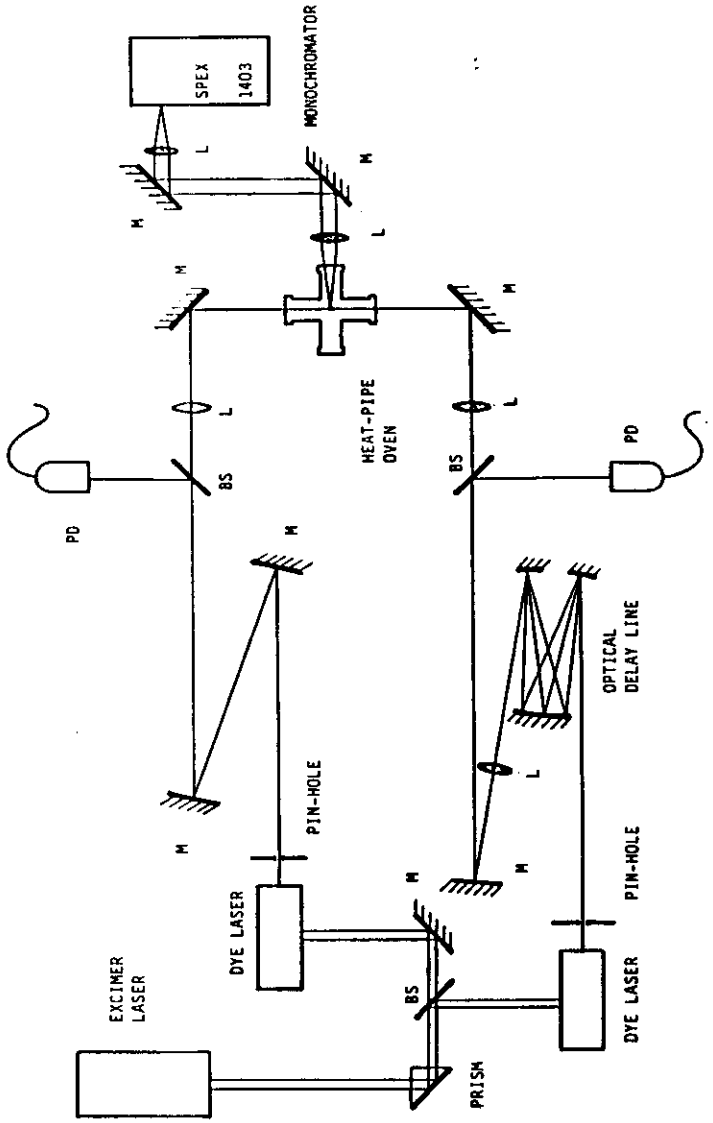

FIG. 2. Experimental setup for the LICET measurement. (PD: photodiode; M: mirror; L: lens; BS: beam splitter)

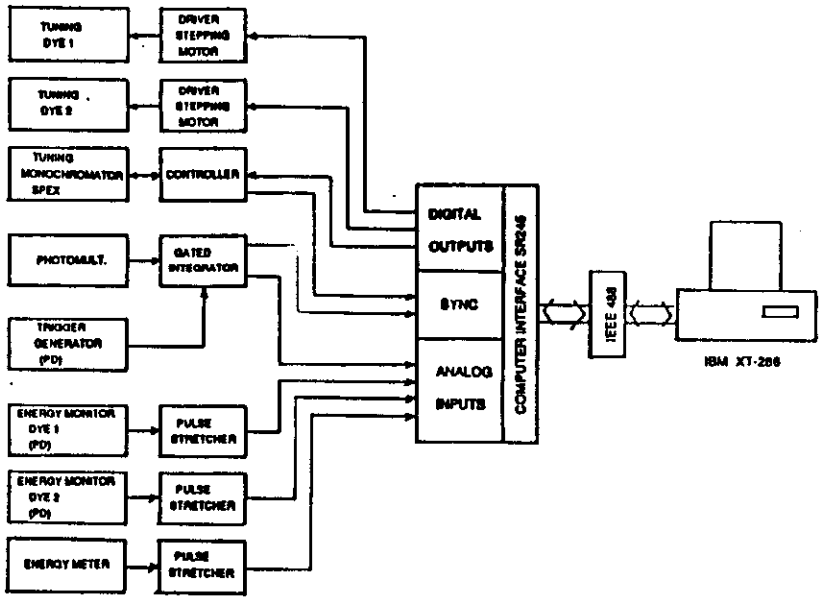

FIG. 3. Data acquisition and control system

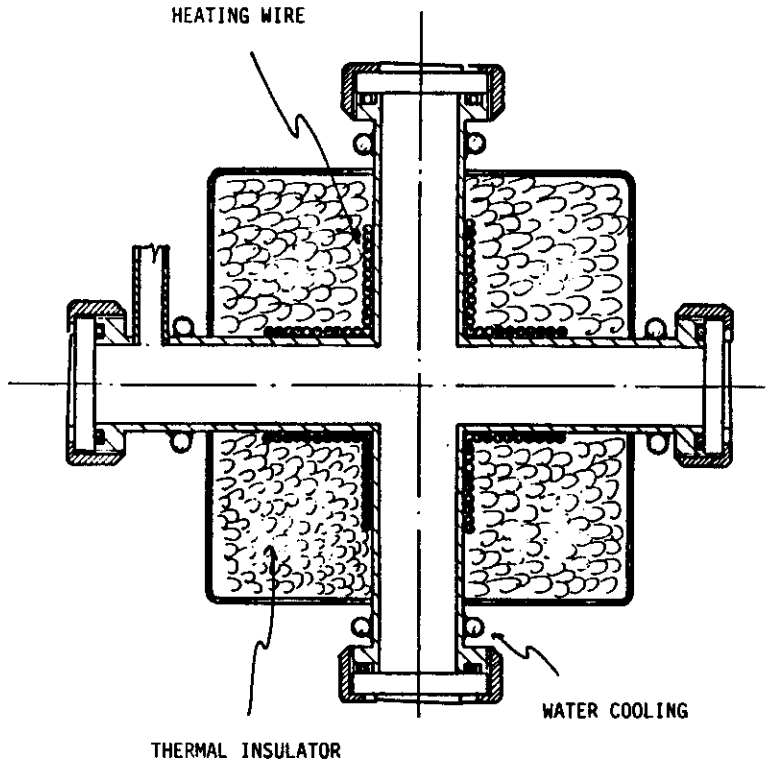

FIG. 4. Mechanical drawing of the heat-pipe oven

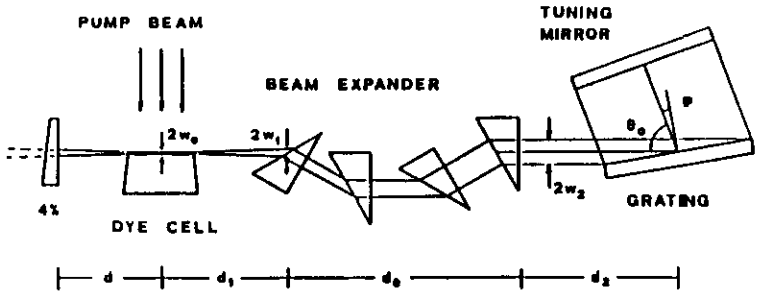

(a)

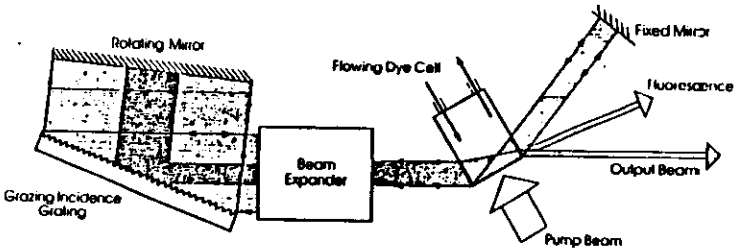

(b)

FIG. 5. (a) Configuration of the dye laser oscillator using a four-prism beam expander; (b) Moya cavity design.

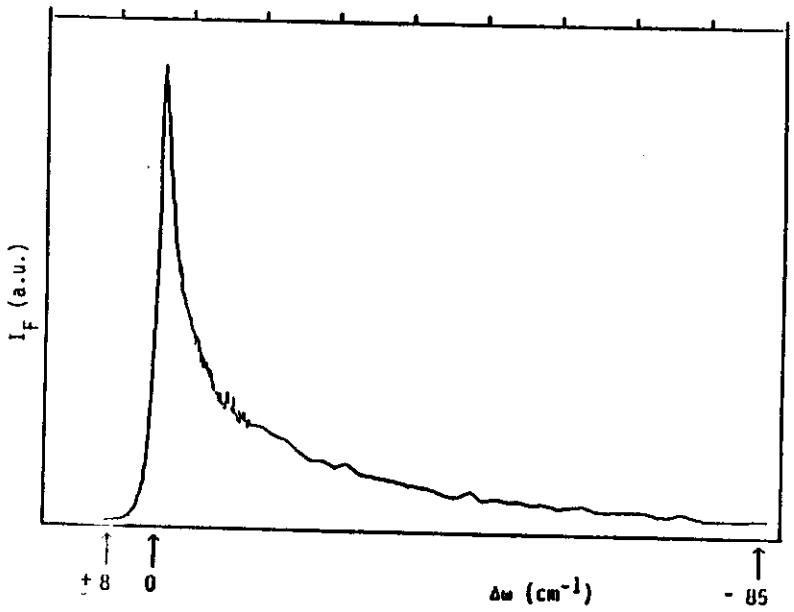

FIG. 6. Spectral profile of the measured LICET process between europium and strontium.

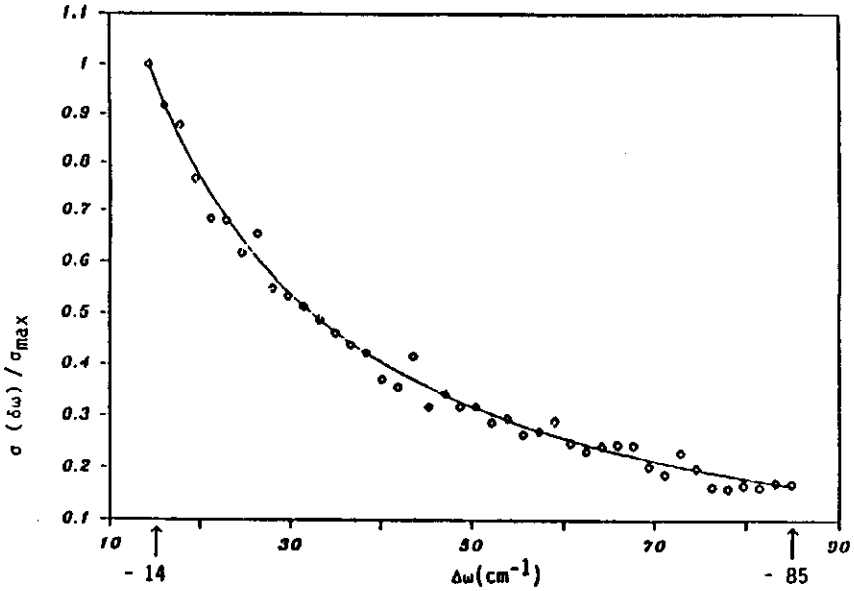

FIG. 7. Line profile in the static wing, measured in the detuning interval -14, -85 cm^{-1}. Experimental points are averages over 30 laser pulses. The continuous line reprents the analytical behavior of the Bambini-Berman model.

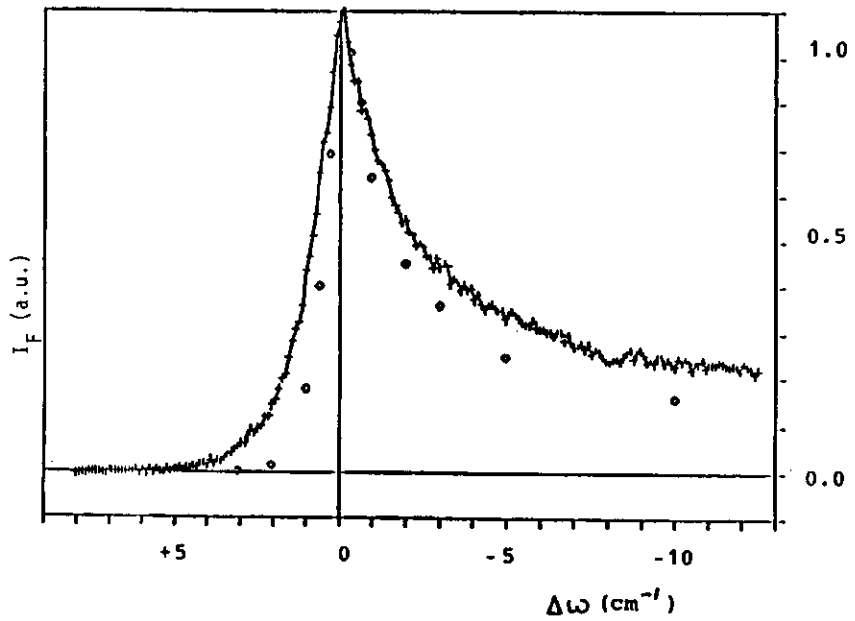

FIG. 8. Line profile in the core region. The circles represent the result of a numerical calculation based on a three-level model.

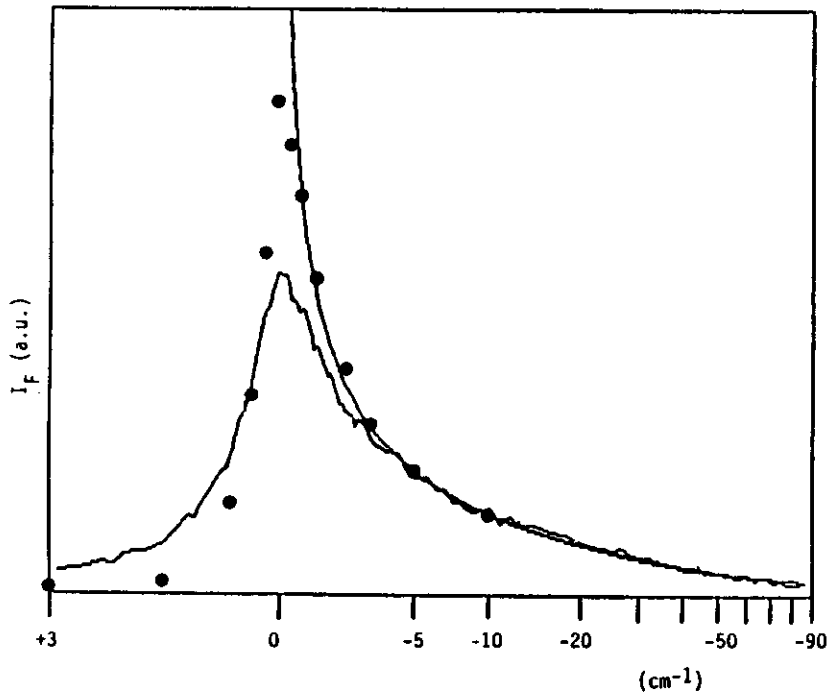

FIG. 9. Spectral profile of the LICET process between Eu and Sr. The frequency scale is compressed logarithmically in order to have a detailed representation in the core region. The continuous line represent the analytical result of the Bambini-Berman model. The circles represent the result of a numerical calculation based on a three-level model.

PHYSICAL REVIEW A VOLUME 36, NUMBER 3 AUGUST 1, 1987

Far-wing study of laser-induced collisional energy transfer

Manlio Matera and Marina Mazzoni
Istituto di Elettronica Quantistica del Consiglio Nazionale delle Ricerche, Via Panciatichi 56/30, I-50127 Firenze, Italy

Roberto Buffa* and Stefano Cavalieri†
Dipartimento di Fisica, Università di Firenze, Largo Enrico Fermi 2, I-50125 Firenze, Italy

Ennio Arimondo
Dipartimento di Fisica, Università di Pisa, Piazza Torricelli 2, I-56100 Pisa, Italy

(Received 27 January 1987)

An experimental study of laser-induced collisional energy transfer in a mixture of europium and strontium vapors is reported. The profile of the excitation spectrum in the static wing has been measured with high accuracy and compared with available calculations, demonstrating that simple two-level models are inadequate to describe the transfer process. A comparison with the predictions of a three-level model assuming dipole-dipole interaction, recently developed by Bambini and Berman, shows for the first time agreement between theory and experiment.

The development of high-power tunable laser sources has prompted in the last decade the study of atomic transitions induced by the simultaneous action of a laser field and a collision. The processes, predicted by Yakovlenko *et al.*,[1] can be described as a reaction of the general form

$$A_i + B_i + \hbar\omega \rightarrow A_f + B_f \ , \tag{1}$$

where $A_{i,f}$ and $B_{i,f}$ are the internal states of the colliding atoms and ω is the laser frequency, close to the difference between the transition frequencies of the atoms. Determination of quasimolecular transient states of the colliding atoms, efficient excitation of high-lying states inaccessible by direct photon absorption, and laser switching of chemical reactions represent the main objectives of the study of laser-induced collisions.

The laser-induced collisional energy transfer (LICET), also designated as radiatively assisted inelastic collision (RAIC), involves an energy transfer from one atom to another with the simultaneous absorption of a photon. Since the first experimental demonstration by Harris and co-workers in a strontium-calcium mixture,[2] radiative collisions have been studied in various binary atomic systems, such as Eu-Sr,[3-5] Rb-K,[6] Na-Ca,[7] and Li-Sr.[8] Among the laser-induced processes, charge transfer,[9] pair absorption,[10] and Penning or associative ionization[11] have been investigated.

The cross section of a LICET process, which is energetically forbidden in the absence of laser field, is maximum when the laser frequency ω is resonant with the frequency ω_0 of the interatomic transition. The line profile, as a function of the laser detuning from line center $\Delta\omega = \omega - \omega_0$, is characterized by an asymmetric shape, showing a gradual falloff on one wing and an abrupt (exponential) falloff on the other. By analogy with the line-broadening theory, the LICET line profile can be divided into an impact and a static region, corresponding to small and large values of $\Delta\omega$, respectively. In the static wing, where the main contributions to the cross section arise from short-range collisions, the profile is strongly affected by the interatomic potentials. In this region, for $|\Delta\omega| \gg 1/\tau_c$, where τ_c is a typical collision time, the process can be described as an instantaneous transition between adiabatic quasimolecular states (quasistatic approximation). From the quasistatic approximation, assuming a dipole-dipole interaction, the LICET cross section in the static wing has been predicted to follow the asymptotic law $|\Delta\omega|^{-1/2}$.[12,13] An asymptotic behavior very close to the $-\frac{1}{2}$ power law is also provided by a numerical resolution of the time-dependent Schrödinger equation for the compound system (atoms+field), under the usual two-level approximation.[14]

High-resolution measurements of the LICET spectrum, performed by Brechignac *et al.* on the Eu-Sr system[4] and by Débarre on the Na-Ca system,[7] have shown that the detuning dependence of the cross section in the static wing can be fitted by a power law $|\Delta\omega|^{\alpha}$ with $\alpha = -0.85$ and $\alpha = -0.8$, respectively. The discrepancy with the theoretical predictions was ascribed to the influence of short-range interactions, including a breakdown of the linear trajectory hypothesis, or to a role played by near-resonant atomic levels.

Recently, a new analysis of the LICET process performed by Bambini and Berman for the Eu-Sr system,[15] has shown that the usual two-level approximation is inadequate to describe accurately the line profile in the far wing. In fact, when the laser detuning $\Delta\omega$ is comparable to the energy defect Δ of the interatomic transition, the initial and intermediate states of the compound system (see Fig. 1) are mixed by the collisional interaction and a three-level treatment is required to describe the transfer process. A similar effect was observed by Niemax in a study of the static wing absorption of the 459.5-nm Eu line collisionally broadened by Sr atoms.[16] Assuming a

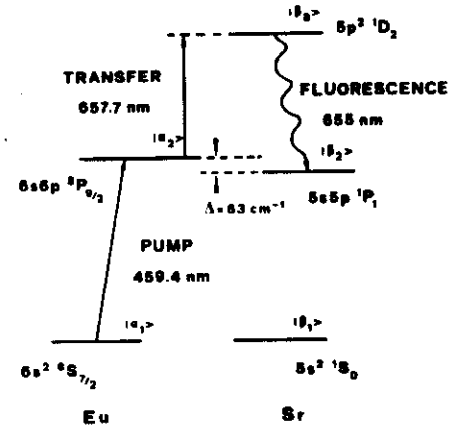

FIG. 1. Energy level diagram for the Eu-Sr laser-induced process. The compound states relevant to the transition are $|\alpha_2\rangle|\beta_1\rangle$ (initial state), $|\alpha_1\rangle|\beta_2\rangle$ (intermediate state), and $|\alpha_1\rangle|\beta_3\rangle$ (final state).

dipole-dipole interaction, the three-level model provides, at first order in the laser field amplitude, the following asymptotic law for the cross section in the static wing:

$$\sigma \propto |\Delta\omega|^{-1/2}(\Delta + |\Delta\omega|)^{-3/2}, \qquad (2)$$

where $\Delta = 63$ cm^{-1} for the Eu-Sr system. This law reduces to the $-1/2$ power law predicted by the quasistatic approximation when $|\Delta\omega| \ll \Delta$ and approaches a -2 power law when $|\Delta\omega| \gg \Delta$.

In this paper a new high-resolution measurement of the far-wing profile for the Eu-Sr system is reported. The experimental setup, described in detail in a previous paper,[17] employed two dye lasers, pumped by the same nitrogen laser, providing 10–50 μJ, 2-nsec pulses with a bandwidth $\simeq 0.1$ cm^{-1}.[18]

The output of one laser (pump laser) was used to populate the Eu($6s6p\ ^8P_{9/2}$) state, while the output of the other laser, delayed by $T \simeq 16$ nsec in order to avoid the direct two-photon excitation of Sr, was used to induce the transfer process. The laser beams were focused into a heat-pipe oven providing the binary vapor mixture, with Eu number densities near 10^{16} atoms/cm^3 and Sr number densities near 10^{17} atoms/cm^3. The population of the final state was monitored by measuring the fluorescence from the Sr($5p\ ^1D_2$) level at $\lambda = 655$ nm. Data acquisition, noise subtraction, monitoring of the energy of the laser pulses, and overall system control were performed by a computer.

A measurement of the LICET spectral profile is shown in Fig. 2. The line-core shape was found to be dependent on the intensity of the transfer laser, proving that the stimulated emission on the Sr($5p\ ^1D_2$)→Sr($5s5p\ ^1P_1$) transition played an important role in the final-state decay. However, the comparison between the line shapes measured at different laser intensities showed that, at the atomic densities of our experiment, stimulated emission

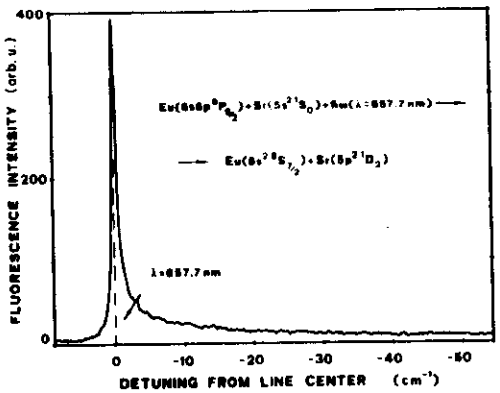

FIG. 2. Spectral profile of the Eu-Sr LICET process versus detuning of the transfer laser $\Delta\omega = \omega - \omega_0$. The spectrum peaks at the wavelength $\lambda = 657.7$ nm, corresponding to the interatomic transition for separated atoms. For experimental conditions see text.

effects were negligible for detunings larger than 5 cm^{-1}. The fluorescence signal measured on the antistatic (blue) side of the resonance revealed the presence of a background process, dependent on the pump laser alone. This background signal was probably due to a pump-laser excitation of high-lying europium levels followed by collisional transfer to strontium populating the Sr($5p\ ^1D_2$) state.

The far-wing profile measured in the detuning interval 6.3–53.2 cm^{-1} is shown in Fig. 3. The fine-tuning system, with a resolution better than 0.1 cm^{-1}, allowed the determination of the detuning from line center with an accuracy of ± 0.3 cm^{-1}. The average energy of the transfer laser, also presented in Fig. 3, remained constant during

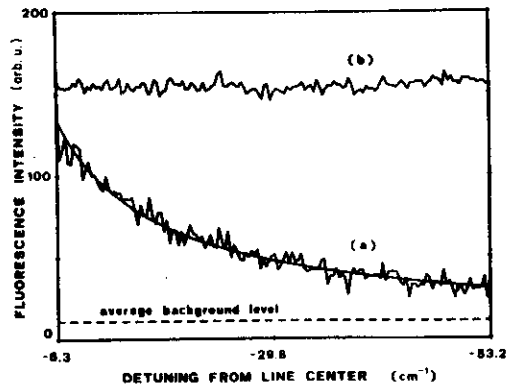

FIG. 3. (a) Line profile in the static wing measured in the detuning interval 6.3–53.2 cm^{-1}. Experimental points are averages over 16 laser pulses. The best fit of Eq. (2) is reported on the data. (b) Transfer laser energy measured during the frequency scanning. The average background level is represented as a dashed line.

the frequency scanning to within 1%.

In order to compare our results with the predictions of the quasistatic theory, the measured far-wing profile was fitted by a power law $|\Delta\omega|^{\alpha}$. The best straight line fitting the log/log plot of the recorded data was found to have a slope $\alpha = -0.79 \pm 0.05$. This value, consistent with the results of the previous high-resolution investigations, confirmed the discrepancy with the quasistatic law $|\Delta\omega|^{-1/2}$ predicted for a dipole-dipole interaction. The uncertainty in the α value arises from a combination of the statistical errors with the systematic errors mainly due to the inaccuracy of the detuning determination. When the fit was performed separately in the detuning intervals 6.3–29.8 cm^{-1} and 29.8–53.2 cm^{-1}, the slopes $\alpha = -0.72 \pm 0.05$ and $\alpha = -1.14 \pm 0.10$ were respectively obtained, proving that the measured profile can be more accurately described by a law with a variable slope.[17]

The analysis of our data showed that the accuracy of the measurement was adequate to the requirements for a quantitative test of theoretical models, making a comparison with the predictions of the three-level theory significant. Therefore, the measured profile in the overall detuning range was fitted with the theoretical law (2). From a two-parameter fit (including a normalization constant) an energy defect $\Delta = 67 \pm 6$ cm^{-1} was estimated, to be compared to the value $\Delta = 63$ cm^{-1} for the Eu-Sr interatomic transition. The corresponding line shape, shown in Fig. 3 as a continuous line through the experimental points, provides a good fit to the data with a small standard deviation. Since the detuning range explored in the experiment was comparable to the Eu-Sr energy defect, the asymptotic slope $\alpha = -2$, predicted by Eq. (2), could not be checked.

The results reported here provide an experimental evidence that the LICET cross section does not follow a simple power law in the static wing, since a significant slope change has been determined in a detuning interval $\simeq 50$ cm^{-1}. Moreover, the experimental results, consistent with the results of previous studies, are in agreement with the predictions of a theoretical model based on a three-level approximation. The deeper insight gained into the dynamics of radiative collisions stimulates further investigation of other types of dipole-dipole laser-induced collisions.

The authors wish to thank Professor R. Pratesi for continuous encouragement, Dr. A. Bambini for helpful discussions, and M. Neri for his valuable technical assistance. This work was performed at the Istituto di Elettronica Quantistica del CNR and was supported by the Ministero della Pubblica Istruzione.

*Present address: Edward L. Ginzton Laboratory, Stanford University, Stanford, CA 94305.
†Present address: Imperial College of Science and Technology, The Blackett Laboratory, Prince Consort Road, London SW7 2BZ, U.K.

[1]L. I. Gudzenko and S. I. Yakovlenko, Zh. Eksp. Teor. Fiz. **62**, 1686 (1972) [Sov. Phys.—JETP **35**, 877 (1972)].
[2]D. B. Lidow, R. K. Falcone, T. F. Young, and S. E. Harris, Phys. Rev. Lett. **36**, 462 (1976).
[3]Ph. Cahuzac and P. E. Toschek, Phys. Rev. Lett. **40**, 1087 (1978).
[4]C. Brechignac, Ph. Cahuzac, and P. E. Toschek, Phys. Rev. A **21**, 1969 (1980).
[5]A. Débarre, J. Phys. B **15**, 1693 (1982).
[6]B. Cheron and H. Lemery, Opt. Commun. **42**, 109 (1982).
[7]A. Débarre, J. Phys. B **16**, 431 (1983).
[8]D. Z. Zhang, B. Nikolaus, and P. E. Toschek, Appl. Phys. B **28**, 195 (1981).
[9]S. E. Harris, J. F. Young, W. R. Green, R. W. Falcone, J. Lukasik, J. C. White, J. R. Willison, M. D. Wright, and G. A. Zdasiuk, in *Laser Spectroscopy*, edited by H. Whalter and R. W. Rothe (Springer-Verlag, New York, 1979), Vol. 4.
[10]J. C. White, R. R. Freeman, and P. F. Liao, Opt. Lett. **5**, 120 (1980).
[11]J. Weiner, J. Chem. Phys. **72**, 2856 (1980).
[12]V. S. Lisitsa and S. I. Yakovlenko, Zh. Eksp. Teor. Fiz. **66**, 1550 (1974) [Sov. Phys.—JETP **39**, 759 (1974)].
[13]A. Gallagher and T. Holstein, Phys. Rev. A **16**, 2413 (1977).
[14]S. E. Harris and J. C. White, IEEE J. Quantum Electron. **13**, 972 (1977).
[15]A. Bambini and P. R. Berman, in *Photons and Continuum States of Atoms and Molecules*, edited by N. K. Rahman, C. Guidotti, and M. Allegrini (Springer-Verlag, Heidelberg, 1987), p. 220.
[16]K. Niemax, Phys. Rev. Lett. **55**, 56 (1985).
[17]M. Matera, M. Mazzoni, R. Buffa, S. Cavalieri, and E. Arimondo, in *Photons and Continuum States of Atoms and Molecules*, edited by N. K. Rahman, C. Guidotti, and M. Allegrini (Springer-Verlag, Heidelberg, 1987), p. 227.
[18]R. Buffa, S. Cavalieri, M. Matera, and M. Mazzoni, Opt. Commun. **58**, 255 (1986).

Analysis of the far-wing behavior in the spectrum of the light-induced collisional-energy-transfer process

A. Agresti
Dipartimento di Fisica, Sezione di Fisica Superiore, via S. Marta 3, I-50139 Firenze, Italy

P. R. Berman
Department of Physics, New York University, 4 Washington Place, New York, New York 10003

A. Bambini and A. Stefanel
Istituto di Elettronica Quantistica del Consiglio Nazionale delle Ricerche, via Panciatichi 56/30, I-50127 Firenze, Italy

(Received 19 October 1987; revised manuscript received 19 February 1988)

The behavior of the quasistatic wing of the light-induced collisional-energy-transfer (LICET) line shape is analyzed. The reaction can be written as $A^* + B + \hbar\Omega \rightarrow A + B^{**}$. The two-level model is found to be inadequate to describe the falloff of the spectral line shape in the quasistatic wing. The three-level model, on the other hand, leads to the prediction of a cross section that depends on the detuning in various ways, according to the strength of the collisional coupling and the influence of the van der Waals shifts on the levels under consideration. Good agreement with existing experimental results is found. To check the approximations made in the derivation of these results, numerical evaluation of the transition probability has been performed for several cases. A Monte Carlo simulation of the full LICET spectrum is also presented.

I. INTRODUCTION

Light-induced collisional energy transfer (LICET) has been studied in the past decade.[1-3] In this process energy is transferred from one atom (previously prepared in an excited state) to another (typically in its ground state) in a gaseous sample via a combined collisional-radiative reaction. The second atom then reaches a highly excited level, having an energy which greatly exceeds that of the initially prepared atom, the energy difference being provided by a photon from a laser field. This reaction can be written as

$$A^* + B + \hbar\Omega \rightarrow A + B^{**} . \tag{1.1}$$

This process is to be distinguished from a two-step process since there is no energy level of atom B resonant with the energy level A^* of atom A. Thus the original excitation energy of atom A and the energy of the photon are simultaneously transferred to atom B in a single quantum-mechanical process of the second order. Several colliding partners were investigated experimentally[4-6] and all of them have shown a sizable transition cross section σ which is obtained when the laser field is tuned near the transition frequency from the initial level of atom A to the final level of atom B. Since this process could, both in principle and in practice, open new possibilities of excitation mechanisms in laser spectroscopy, a great deal of theoretical work has been devoted to the study of the detailed dynamics of these transitions.[3,7-9] It appeared that this process could also lead to the determination of interatomic potentials at large-to-average interatomic separations, since the wing of the LICET spectrum can serve as a direct measure of the potentials.[7] In a typical situation where the van der Waals interaction dominates at large interatomic separation, it was found that the LICET excitation spectrum, in its simplest formulation as a two-level transition, had to follow a power-law dependence of the type

$$\sigma(\Delta) \sim |\Delta|^{-1/2} \tag{1.2}$$

when the laser frequency was detuned by the amount Δ from resonance for the overall LICET reaction.

This behavior was not confirmed in all experiments. In the case of Eu-Sr colliding partners the wing of the LICET spectrum was found to follow the power law

$$\sigma(\Delta) \sim |\Delta|^{-0.85} \tag{1.3}$$

whereas, in the case of Na-Ca, the wing was found to go to zero with the law

$$\sigma(\Delta) \sim |\Delta|^{-0.00} . \tag{1.4}$$

The main cause of the departure of the experimental results from the theoretical predictions was found[10,11] to lie in the wrong assumption that the LICET transition may always be described as a two-level transition. When this assumption is removed, and replaced by a more realistic assumption of a three-level transition, a new picture of the process emerges. The transition is then best described by a transfer of energy from a doublet of quasimolecular levels dressed by the interatomic collisional interaction to a final state.

In this case, one finds that the far wing of the spectrum falls to zero as

$$\sigma(\Delta) \sim |\Delta|^{-1/2}(\omega + |\Delta|)^{-3/2} , \tag{1.5}$$

where ω is the frequency difference of the doublet of quasimolecular states at infinite interatomic separation (i.e., with no collisional interaction). The law (1.5) predicts that the local slope of the wing varies with Δ, in contrast to the single-slope behavior (1.3) or (1.4) estimated from the experimental data. Still, it agrees fairly well with (1.3) [or (1.4)] when the appropriate value of ω is used: differences between (1.5) and (1.3) [or (1.4)] can hardly be detected due to the insufficient precision of the experimental data. Moreover, recent experiments performed with greater accuracy[12] have shown evidence of a two-slope behavior in the wing of the LICET spectrum.

In this paper we analyze the new model and discuss its results in detail. All the relevant features found from previous models are retrieved as special cases when the transition can be described as a true two-level transition. Results of numerical calculations are shown which confirm the validity of the approximations used in the work. It is also shown that the transition probability is not greatly affected by other levels than those considered in this paper. Finally, two particular cases of excitation schemes, differing by the order in which the transition processes occur, are shown to lead to the same far-wing behavior of the spectrum given by (1.5).

This paper is organized as follows. In Sec. II the model is described in detail and the cross section for the transition in the far wing is derived. Section III presents the computer calculations that were performed to show the validity of the assumptions made. Transition probabilities for some range of the impact parameter and the full spectrum of the LICET process for the case of Eu-Sr colliding partners, evaluated by means of a Monte Carlo technique, are shown. Section IV is devoted to a discussion of the results and a comparison with experimental data. In Appendix A we discuss the conditions of validity for the method of stationary phase used to derive an analytical expression for the cross section in the quasistatic wing. In Appendix B we show some results for the transition probability in a different scheme of excitation. Finally, numerical results for processes with more than three levels are shown in Appendix C.

II. THE MODEL

A. The equations for the level amplitudes

In Fig. 1 the energy-level configuration of the atoms undergoing a LICET process is shown. There are other possible configurations as well (see for instance Ref. 9). Another scheme of energy levels is worked out in Appendix B.

Atom A enters the collision in an excited state α^* while atom B is in its ground state. During the collision the excitation energy of atom A is transferred to atom B with the simultaneous absorption of a photon from a laser field. At the end of the collisional interaction atom B is in its excited state β^{**}, while A is left in its ground state.

If an excited level β^* of atom B is nearly resonant with the energy level α^* in which atom A is initially prepared as shown in Fig. 1, then one channel of excitation dominates the LICET reaction. This channel is characterized by transfer of the excitation energy of atom A to atom B through a collisional interaction, followed by absorption of a photon from the laser field to bring atom B to state β^{**}. State β^* of B should not be resonant with state α of atom A, otherwise the transition would involve a two step excitation. We use as basis states the compound atom states. Thus, with reference to Fig. 1, the basis state vectors are

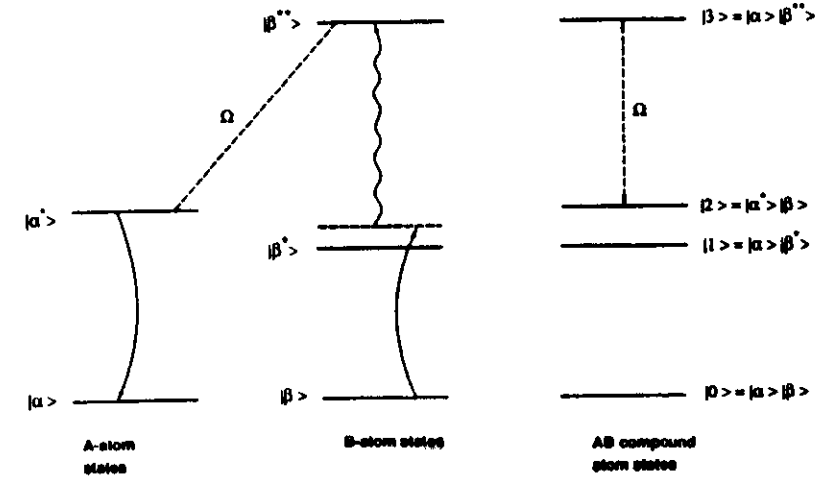

FIG. 1. Energy-level scheme for a LICET reaction. On the left side the energy levels of the separate atoms are shown. The LICET transition occurs from state α^* of atom A to state β^{**} of atom B. The field frequency Ω is such that $\hbar\Omega = E_3 - E_2$. On the right side, the compound atomic states are shown.

$$|1\rangle=|\alpha\rangle|\beta^*\rangle\ , \tag{2.1a}$$

$$|2\rangle=|\alpha^*\rangle|\beta\rangle\ , \tag{2.1b}$$

$$|3\rangle=|\alpha\rangle|\beta^{**}\rangle\ . \tag{2.1c}$$

We make several assumptions before writing down the equations of motion for the state amplitudes.

First we consider the laser field to be classical, and evaluate the transition cross section to the lowest order in the field. The electric field is also assumed to be constant during each collision, since the latter takes place on a time scale of the order of 10^{-12} sec, much shorter than the typical time scale for the variations of the laser pulses.

We also assume that the translational degrees of freedom are not affected by the transition process. When the laser field is detuned from the interatomic resonance, the energy defect (or excess) must be supplied by (transferred to) the translational degrees of freedom, but we assume that this is a negligible fraction of the total kinetic energy in the process. Moreover, we suppose that the atoms follow classical, straight-line trajectories during a collision. Thus the interatomic separation is expressed at any time by the (classical) variable R,

$$R=(b^2+v^2t^2)^{1/2}\ . \tag{2.2}$$

The magnetic sublevels degeneracy is also ignored.

The equations of motion for the amplitudes of the states (2.1a and 2.1b) are then written as

$$i\dot{c}_1=S_1c_1+V_{12}(t)e^{-i(\omega_2-\omega_1)t}c_2+\chi e^{-i(\omega_3-\omega_1-\Omega)t}c_3\ , \tag{2.3a}$$

$$i\dot{c}_2=S_2c_2+V_{21}(t)e^{-i(\omega_1-\omega_2)t}c_1\ , \tag{2.3b}$$

$$i\dot{c}_3=S_3c_3+\chi e^{-i(\omega_1-\omega_3+\Omega)t}c_1\ . \tag{2.3c}$$

In Eqs. (2.3) S_j denote the shifts induced on the jth level by the collisional interaction. The dominant shifts are those caused by the dipole-dipole interaction, for which S_j take the form

$$S_j=C_j/R^6\quad (j=1,2,3)\ . \tag{2.4}$$

The $V_{12}(t)$ and the χ terms denote the collisional interaction and the atom-field interaction, respectively. We see that $V_{12}(t)$ couples directly the state $|1\rangle$ to the state $|2\rangle$. The explicit form of $V_{12}(t)$ depends on the particular interaction potential between the two atoms. For instance, if state α and state α^* of atom A are coupled by a dipole transition, and also state β and state β^* of atom B are coupled by a dipole transition, then the compound states $|1\rangle$ and $|2\rangle$ are coupled by a dipole-dipole transition with $V_{12}(t)$ given by

$$V_{12}(t)=\frac{\mathcal{V}_0}{R^3}\ . \tag{2.5}$$

The quantity V_{12} depends on the time t through the explicit time dependence of the classical parameter R given by (2.2).

Because of the assumptions made above, χ is constant during the collisional interaction. Of the two components of the electromagnetic field, only the one that makes the interaction term slowly time varying has been retained (rotating wave approximation).

To obtain the cross section for the transition process, one should first integrate system (2.3) with the initial conditions

$$c_1(-\infty)=0\ , \tag{2.6a}$$

$$c_2(-\infty)=1\ , \tag{2.6b}$$

$$c_3(-\infty)=0 \tag{2.6c}$$

to obtain the probability $|c_3|^2$ for exciting atom B to state β^{**}, and then average this result over all possible collisional configurations (namely, over the impact parameter b and relative speed v).

B. Perturbative solution of the equations of motion

We pass now to the Schrödinger representation of the Eq. (2.3), and choose the energy of the initial level as the reference level. By means of the transformations

$$a_1=c_1\exp[i(\omega_2-\omega_1)t]\ , \tag{2.7a}$$

$$a_2=c_2\ , \tag{2.7b}$$

$$a_3=c_3\exp[i(\omega_2-\omega_3)t]\ , \tag{2.7c}$$

Eq. (2.3) now read

$$i\dot{a}_1=(\omega_1-\omega_2)a_1+S_1a_1+V_{12}a_2+\chi e^{i\Omega t}a_3\ , \tag{2.8a}$$

$$i\dot{a}_2=S_2a_2+V_{21}a_1\ , \tag{2.8b}$$

$$i\dot{a}_3=(\omega_3-\omega_2)a_3+S_3a_3+\chi e^{-i\Omega t}a_1\ . \tag{2.8c}$$

Equations (2.8) can be simplified if we consider that, to first-order perturbation theory in the field amplitude, the final level a_3 has very little population during and after the collisional interaction. We can therefore omit the term $\chi e^{i\Omega t}a_3$ in Eq. (2.8a), which would induce population from level a_3 to flow back to level a_1.

This approximation leads to the decoupling of the first two equations from the third. Setting $\omega=\omega_2-\omega_1$, we can write

$$i\dot{\mathbf{a}}=\underline{A}\,\mathbf{a}\ , \tag{2.9}$$

where

$$\mathbf{a}=\begin{bmatrix}a_1\\a_2\end{bmatrix},\quad \underline{A}=\begin{bmatrix}-\omega+S_1 & V_{12}\\ V_{21} & S_2\end{bmatrix}. \tag{2.10}$$

In some cases, the frequency difference $\omega_2-\omega_1$ between level 2 and level 1 can be considered large enough that the state a_1 behaves as a virtual level. If this is the case, then the far wing of the LICET spectrum falls to zero with a constant slope $-\frac{1}{2}$, as is shown below. Two conditions are to be met for state a_1 to be a virtual state. The collisional interactions must vary slowly compared to the inverse of the frequency difference $\omega_2-\omega_1$,

$$\left|\frac{\dot{V}_{12}}{V_{12}}\right|\ll|\omega_2-\omega_1|\ . \tag{2.11}$$

This means that there is no Fourier component in the spectrum of the collisional interaction potential that matches the frequency difference between level 1 and level 2, so that no population transfer can take place between them.

The second condition is that the interaction itself must be a small perturbation with respect to the same frequency difference,

$$|V_{12}|\ll|\omega_2-\omega_1|\ . \tag{2.12}$$

There are situations in which only the first condition is satisfied. For instance, in cases in which we measure the spectrum at detunings from resonance that are comparable with the frequency difference $\omega_2-\omega_1$ we are probing collisions that occur at small interatomic distances, for which the level shift induced by the collision matches the detuning, i.e.,

$$\frac{|V_{12}|^2}{|\omega_2-\omega_1|}\sim|\Delta|\ . \tag{2.13}$$

In such situations, the collisional interaction $V_{12}(R)$ becomes comparable with the frequency difference $|\omega_2-\omega_1|$. Still, the time scale over which V_{12} varies is of the order of b/v, and may be large with respect to $|\omega_2-\omega_1|^{-1}$, so that (2.11) is satisfied, but (2.12) is not.

To treat a situation in which (2.11) only is satisfied, we assume that the matrix $\underline{A}$ is constant in one period $1/|\omega_2-\omega_1|$, and look for the time evolution of the system on the same time scale. The matrix $\underline{A}$ can be diagonalized by the transformation

$$\underline{T}\underline{A}\underline{T}^{-1}=\underline{D}\equiv\begin{bmatrix}\lambda_1 & 0\\ 0 & \lambda_2\end{bmatrix}, \tag{2.14}$$

where $\underline{T}$ takes the form

$$\underline{T}=\begin{bmatrix}\cos\theta & -\sin\theta\\ \sin\theta & \cos\theta\end{bmatrix} \tag{2.15}$$

and the eigenvalues λ_1,λ_2 are given by

$$\lambda_1=\tfrac{1}{2}\{S_1+S_2-\omega-[(S_2-S_1+\omega)^2+4V_{12}^2]^{1/2}\}\ , \tag{2.16a}$$

$$\lambda_2=\tfrac{1}{2}[S_1+S_2-\omega+[(S_2-S_1+\omega)^2+4V_{12}^2]^{1/2}]\ . \tag{2.16b}$$

We find, after some manipulations,

$$\sin(\theta)=\left|\frac{1}{2}\left\{1-\frac{\delta}{(\delta^2+V_{12}^2)^{1/2}}\right\}\right|^{1/2}, \tag{2.17a}$$

$$\cos(\theta)=\left|\frac{1}{2}\left\{1+\frac{\delta}{(\delta^2+V_{12}^2)^{1/2}}\right\}\right|^{1/2}, \tag{2.17b}$$

where δ is given by

$$\delta=\frac{\omega_2+S_2-\omega_1-S_1}{2}\equiv\frac{\omega+S_2-S_1}{2} \tag{2.18}$$

[δ is assumed positive; otherwise change the sign in (2.16) and (2.17)]. On the same time scale the vector b defined by the transformation

$$\mathbf{b}\equiv\begin{bmatrix}b_1\\b_2\end{bmatrix}=\underline{T}\mathbf{a} \tag{2.19}$$

transforms according to the equation

$$i\dot{\mathbf{b}}=\underline{D}\mathbf{b}\ . \tag{2.20}$$

On a larger time scale, b evolves according to

$$i\dot{\mathbf{b}}=\begin{bmatrix}\lambda_1 & -i\dot{\theta}\\ i\dot{\theta} & \lambda_2\end{bmatrix}\mathbf{b}\ . \tag{2.21}$$

In view of the slow time variation of V_{12}, the term $\dot{\theta}$ is always small when compared to $\lambda_2-\lambda_1$, so that we can ignore the transitions induced by the off diagonal terms in (2.21) between the two levels b_1 and b_2.

The components b_1 and b_2 of the vector b are the amplitudes of the quasimolecular states a_1 and a_2 dressed by the collisional interaction V_{12}. They can be found by integrating (2.21), if we neglect the off-diagonal terms. We find

$$b_1(t)\approx0\ , \tag{2.22a}$$

$$b_2(t)\approx\exp\left\{-i\int_{-\infty}^{t}\lambda_2(t')dt'\right\}. \tag{2.22b}$$

We note that no real population transfer occurs between a_1 and a_2, since at $t=+\infty$ the collisional interaction goes to zero, and the dressed states b_1 and b_2 coincide with a_1 and a_2. Thus

$$a_1(+\infty)=b_1(+\infty)=0\ . \tag{2.23}$$

However, during the interaction, a_1 may get an appreciable fraction of the total population. We find

$$a_1(t)=\cos(\theta)b_1+\sin(\theta)b_2\approx\sin(\theta)\exp\left\{-i\int_{-\infty}^{t}\lambda_2(t')dt'\right\}. \tag{2.24}$$

Note that $\sin(\theta)$ at finite times may be of the same order of magnitude as $\cos(\theta)$ if the collisional interaction V_{12} is comparable to, or even larger than, the instantaneous frequency difference (including possible van der Waals shifts) between the two states. In other words, the composite atomic state a_1 is populated during the collision, but the quasimolecular state b_1 enters the problem as a true virtual state whose population is always negligibly small.

Substituting (2.24) for a_1 in Eq. (2.8c) and integrating, we obtain the following expression for the probability amplitude of the final level (to first-order perturbation theory):

$$a_3(t)=-i\chi\exp\left|-i\left|(\omega_1-\omega_2)t+\int_{-\infty}^{t}S_3dt'\right|\right|\int_{-\infty}^{t}dt'\sin(\theta)\exp\left\{-i\Delta t'+i\int_{-\infty}^{t'}(S_3-\lambda_2)dt''\right\}, \tag{2.25}$$

where Δ is the detuning of the laser frequency from the interatomic resonance

$$\Delta=\Omega-(\omega_3-\omega_2)\ . \tag{2.26}$$

Equation (2.25) is valid when the collisional interaction has a slow rate of change and condition (2.11) is valid. If condition (2.12) is also satisfied, then Eq. (2.25) can be simplified to

$$a_3(t)=-\frac{iX}{2}\exp\left\{-i\left[(\omega_3-\omega_2)t+\int_{-\infty}^{t}S_3dt'\right]\right\}\int_{-\infty}^{t}dt'\frac{V_{12}}{\delta}\exp\left[-i\Delta t'+i\int_{-\infty}^{t'}\left[S_3-S_2-\frac{V_{12}}{2\delta}\right]dt''\right]\ . \tag{2.27}$$

The cross section for the LICET process is then evaluated, using (2.25) or (2.27), as

$$\sigma(\Delta)=2\pi\int_0^\infty db\,b\,(\,|a_3(+\infty)|^2)_v\ , \tag{2.28}$$

in which the averaging process over the impact parameter b and the relative speed v is carried out.

C. The far wing of the LICET spectrum

In this section we use the method of stationary phase to approximately evaluate the final-state probability amplitudes [Eqs. (2.25) or (2.27)], to be used in the expression (2.28) for the cross section. This method applies only for large values of $|\Delta|$ in the quasistatic wing of the spectrum. Details of the validity conditions are found in Appendix A. Points of the stationary phase occur whenever the incident photon frequency equals the transition frequency between quasimolecular levels 2 and 3, that is, when

$$\hbar\Omega=[E_3+\hbar S_3(R_s)]-[E_2+\hbar\lambda_2(R_s)]$$

or

$$\Delta=S_3(R_s)-\lambda_2(R_s)\ , \tag{2.29}$$

where R_s indicates the point at which the phase is stationary.

For the atomic level configuration shown in Fig. 1, λ_2 is always positive during the collision, i.e., the instantaneous energy of the dressed state b_2 is higher than the unperturbed energy ω_2, which has been chosen as the reference energy ($\omega_2=0$). Moreover, in general, the shift S_3 of the final level (be it negative or positive) is smaller than λ_2, since the latter is induced by the much stronger collisional interaction with the state a_1 which lies very close in energy to a_2. Thus, in the present configuration, we do expect that the wing of the LICET spectrum extends towards the red region ($\Delta<0$). Collisions that occur with an impact parameter greater than R_s do not contribute significantly to the probability amplitude of the final level. Thus the measurement of the far wing of the spectrum is a probe for collisions occurring at small interatomic distance.

For the collisions that occur with an impact parameter smaller than R_s, we have two points of stationary phase. The contributions to the integral in (2.25) in these two points add up to give

$$|a_3(+\infty)|^2=\chi^2\left|\sin\theta_s\left|\frac{2\pi}{|\ddot{\phi}_s|}\right|^{1/2}\left\{\exp\left[i\left[+\frac{\pi}{4}+\phi_+\right]\right]+\exp\left[i\left[-\frac{\pi}{4}+\phi_-\right]\right]\right\}\right|^2\ , \tag{2.30}$$

where

$$|\ddot{\phi}_s|=\left|\frac{d}{dt}(\Delta-S_3-\lambda_2)\right|_{R=R_s}=\left|\left\{-\frac{6C_3}{R_s^7}+\mathcal{D}^{-1}\left[\frac{6C_1}{R_s^7}\left[\frac{C_3}{R_s^6}-\frac{C_2}{R_s^6}-\Delta\right]+\frac{6C_2}{R_s^7}\left[\frac{C_3}{R_s^6}-\frac{C_1}{R_s^6}+\omega-\Delta\right]-\frac{2p\mathcal{V}_0^2}{R_s^{2p+1}}\right]v\left[1-\frac{b^2}{R_s^2}\right]^{1/2}\right\}\right|\ , \tag{2.31}$$

and

$$\mathcal{D}=|\omega-S_1+S_2+2S_3-2\Delta|\ , \tag{2.32}$$

$$|\sin(\theta_s)|=\mathcal{D}^{-1}|S_3-S_2-\Delta|\ . \tag{2.33}$$

In Eq. (2.31) we have used explicitly the fact that the shifts of the levels are dominated by the van der Waals interaction, which leads to the expression (2.4). The collisional interaction, on the other hand, has been retained in its general form,

$$V_{12}(R)=\frac{\mathcal{V}_0}{R^p}\ , \tag{2.34}$$

with $p=3$ for a dipole-dipole interaction and $p=4$ for a quadrupole-dipole interaction.

The two terms

$$\exp\left[i\left[\frac{\pi}{4}+\phi_+\right]\right]$$

and

$$\exp\left[i\left[-\frac{\pi}{4}+\phi\right]\right]$$

come from the two points at which stationary phase is reached. They determine interference in the build up of population $|a_3|^2$ at $t=+\infty$, as will be shown later when we show explicit calculations for $|a_3|^2$ at varying impact parameters. If we ignore these interference effects, and substitute its average value 2 for the expression

$$\left|\exp\left[i\left[\frac{\pi}{4}+\phi_+\right]\right]+\exp\left[i\left[-\frac{\pi}{4}+\phi_-\right]\right]\right|^2\ ,$$

we can find simple formulas for the cross section in several cases of interest. We will see that the elimination of the interference effects does not introduce significant errors in the determination of the cross section.

We discuss now several cases. In what follows, the atomic energy level configuration is of the type shown in Fig. 1. Thus $\omega=\omega_2-\omega_1$ is positive and a stationary phase condition is reached only for $\Delta<0$.

1. Dipole-dipole interaction, negligible van der Waals shifts

In this case, $p=3$ in (2.34), and $S_1=S_2=S_3=0$. This case has been already discussed in a previous paper, and we report here the results only for completeness.

The interatomic distance at which stationary phase occurs can be evaluated from (2.16a) and (2.29). We find

$$R_s=\left|\frac{\mathcal{V}_0^2}{\Delta^2-\omega\Delta}\right|^{1/6}\quad(\Delta<0)\ . \tag{2.35}$$

The transition probability is then given by

$$|a_3(+\infty)|^2=\frac{4\pi^2\chi^2(-\Delta)R_s^7}{6\mathcal{V}_0^2v(1-b^2/R_s^2)^{1/2}}\ . \tag{2.36}$$

Substituting the average relative speed $\bar{v}$ for v in (2.28) and integrating over the impact parameter, we find

$$\sigma(\Delta)=\tfrac{4}{3}\pi^2\frac{\chi^2(-\Delta)R_s^9}{\bar{v}\mathcal{V}_0^2}\quad(\Delta<0) \tag{2.37}$$

and, using (2.35),

$$\sigma(\Delta)=\tfrac{4}{3}\pi^2\frac{\chi^2\mathcal{V}_0}{|\Delta|^{1/2}(\omega+|\Delta|)^{3/2}}\quad(\Delta<0)\ . \tag{2.38}$$

This is the formula that has been derived in Refs. 10 and 11. We note that the cross section falls to zero with a local slope that varies from 0.5 when $|\Delta|\ll\omega$ to 2 when $|\Delta|\gg\omega$. If the average slope in some interval is measured, one may find any intermediate value, depending on the extension of the interval with respect to the frequency defect ω.

2. Dipole-dipole interaction, nonvanishing van der Waals shifts

We consider now the case in which one level, say level 1, has a large van der Waals shift of the same order of magnitude as V_{12}^2/δ at the typical interatomic separation at which transition occurs. We need now to retain its contribution in the evaluation of $|\ddot{\phi}_s|$, Eq. (2.31). We find that the point at which the stationary phase occurs is now

$$R_s=\left|\frac{\mathcal{V}_0^2-C_1\Delta}{\Delta^2-\omega\Delta}\right|^{1/6}\ . \tag{2.39}$$

A further restriction on C_1 arises because of our requirement that

$$\Delta E=\hbar(\lambda_2-\lambda_1) \tag{2.40}$$

must be large when compared to $\hbar\dot{\theta}$. This would be violated if C_1 were large and positive. Thus we restrict our discussion to the case of negative C_1. From (2.39), with $C_1<0$ and $\Delta<0$, we see that the interatomic distance R_s at which the stationary phase occurs decreases very rapidly when $|\Delta|$ increases, and the cross section in the wing follows the behavior

$$\sigma(\Delta)=\tfrac{4}{3}\pi^2\frac{\chi^2(\mathcal{V}_0^2-C_1\Delta)^{1/2}}{\bar{v}|\Delta|^{1/2}(\omega+|\Delta|)^{3/2}}\ . \tag{2.41}$$

In those regions in which

$$|\Delta|>\frac{\mathcal{V}_0^2}{|C_1|}\ , \tag{2.42}$$

the laser detuning cannot be matched by the level shift difference (i.e., there is no point of stationary phase), and the cross section becomes negligibly small.

In a previous paper[13] computer calculations were performed on the three-level system, with an energy-level scheme like the one shown in Fig. 1, and using a large, negative value for the van der Waals shift of level 1. The far-wing spectrum was found to fall off to zero very rapidly, according to the discussion above.

Another behavior is found in the case in which the relevant van der Waals shift is that of level 2. We find that the point of stationary phase occurs at

$$R_s=\left|\frac{\mathcal{V}_0^2+C_2(\omega-\Delta)}{\Delta^2-\omega\Delta}\right|^{1/6}\ . \tag{2.43}$$

We require now that $C_2>0$ since there must be no level crossing for our model to be valid.

The cross section in its far wing will then follow the law

$$\sigma(\Delta)=\tfrac{4}{3}\pi^2\frac{\chi^2(\mathcal{V}_0^2+2C_2\omega)}{[\mathcal{V}_0^2+C_2(\omega-\Delta)]^{1/2}}\frac{1}{|\Delta|^{1/2}(\omega+|\Delta|)^{3/2}}\ . \tag{2.44}$$

In this case the laser detuning can always be matched at some point by the level shift difference (R_s is always greater than C for any negative Δ), so that there will be no sharp cutoff of the cross section. The latter will eventually fall to zero with the law

$$\sigma(\Delta)\sim|\Delta|^{-0.5}(\omega+|\Delta|)^{-2} \tag{2.45}$$

when $\omega+|\Delta|$ becomes larger than $\mathcal{V}_0^2/C_2$.

3. Dipole-quadrupole interaction, nonvanishing van der Waals shift

When the interaction between level 1 and level 2 is a dipole-quadrupole interaction ($p=4$), the van der Waals shifts are dominant over the term $\mathcal{V}_0^2/R_z^9$ in Eq. (2.31), and they cannot be neglected. In this case, the point at which stationary phase occurs is given by the solution of the full Eq. (2.29); that is rewritten here explicitly as

$$\Delta=\frac{C_3}{R_z^4}-\frac{1}{2}\left|\frac{C_1+C_2}{R_z^6}-\omega\right| -\frac{1}{2}\left|\left|\frac{C_2-C_1}{R_z^6}+\omega\right|^2+\frac{4\mathcal{V}_0^2}{R_z^8}\right|^{1/2} . \tag{2.46}$$

The resulting line shape in the wing is rather complicated and will not be reported here.

So far, we have seen that, when the transition takes place from a doublet of collisionally dressed, quasimolecular states to a single final state, the far wing of the spectrum may have one of several possible line shapes, depending on the values of the parameters C_j involved in the process. All these line shapes merge into either of two (simple) line shapes (one for the case $p=3$, one for the other case $p=4$) when the intermediate level (level 1 in the energy-level scheme of Fig. 1) is a true virtual level, i.e., it is negligibly populated at any time during the collision. This will certainly occur when both conditions (2.11) and (2.12) are satisfied at any time during the collision.

We treat now this limit case, which applies when the frequency difference ω between levels 1 and 2 is much larger than the van der Waals shifts, the collisional interaction, and the frequency detuning of the laser field. These results have been derived earlier by several authors.[7-9]

4. Limit case

(a) Dipole-dipole interaction in the limit $\omega \gg |S_j|$, $\omega \gg |V_{12}|$, $\omega \gg |\Delta|$. In this case $p=3$, and the contribution V_{12}^2/ω adds to S_2 to form the total van der Waals shift of the initial level 2 (level 1 now acts as a virtual level, similar to all other levels that induce a van der Waals shift on level 2),

$$S_2^{(t)}=S_2+\frac{V_{12}^2}{\omega}\equiv\frac{C_2^{(t)}}{R_z^6} \tag{2.47}$$

(2δ is now equal to ω because of our assumptions). Since both conditions (2.11) and (2.12) are satisfied, Eq. (2.27) can be used to find $|a_3(+\infty)|^2$. We apply again the method of the stationary phase to find an approximate value for $|a_3|^2$, in the far wing of the spectrum.

Formally, this value can still be written in the form 2.30), but now $|\ddot{\phi}_z|$ and $\sin(\theta_z)$ have a different expression [obtainable from (2.31) and (2.33), respectively in the limit $\omega \to \infty$]

$$|\ddot{\phi}_z| \to \frac{6v(1-b^2/R_z^2)^{1/2}}{R_z^7}|C_2^{(t)}-C_3| , \tag{2.48}$$

$$\sin(\theta_z) \to \frac{1}{\omega^2}\mathcal{V}_0^2/R_z^6 . \tag{2.49}$$

The stationary phase occurs at R_z given by the solution of the equation

$$\Delta=\frac{C_3-C_2^{(t)}}{R_z^6} . \tag{2.50}$$

Notice that, in this limit case, the point at which stationary phase occurs (i.e., the point where the instantaneous frequency difference matches the laser frequency) is entirely determined by the shifts induced on levels 2 and 3 by other virtual levels, while the amplitude of the transition is determined by the collisional interaction V_{12}^2.

Using (2.48)-(2.50), we find (again neglecting interference between the two points along the trajectory at which stationary phase occurs)

$$|a_3(+\infty)|^2=\frac{4\pi^2\chi^2}{\omega^2}\frac{\mathcal{V}_0}{R_z^6}\frac{R_z^7}{6v(1-b^2/R_z^2)^{1/2}} \times\frac{1}{|C_2^{(t)}-C_3|} , \tag{2.51}$$

which gives, after averaging over b and v,

$$\sigma(\Delta)=\frac{4\pi^2\chi^2}{3v}\frac{\mathcal{V}_0^2}{\omega^2|C_2^{(t)}-C_3|}\frac{1}{|\Delta|^{1/2}} , \tag{2.52}$$

which agrees with the far-wing behavior predicted by the theories based upon a two-level model.

(b) Dipole-quadrupole interaction in the limit $\omega \gg |S_j|$, $\omega \gg |V_{12}|$, $\omega \gg |\Delta|$. In this case, the point at which stationary phase occurs is given by the same equation (2.50), as discussed above. The $|\ddot{\phi}_z|$ term is also given by (2.49). What changes in this case is the factor $\sin(\theta_z)$, which gives the amplitude of the transition,

$$\sin^2(\theta_z)=\frac{1}{\omega^2}\frac{\mathcal{V}_0^2}{R_z^8} . \tag{2.53}$$

The probability $|a_3|^2$ at $t=+\infty$ is given by

$$|a_3(+\infty)|^2=\chi^2\frac{4\pi^2}{6v(1-b^2/R_z^2)^{1/2}}\frac{R_z^7}{|C_2-C_3|}\frac{1}{\omega^2}\frac{\mathcal{V}_0^2}{R_z^8} , \tag{2.54}$$

which yields the cross section

$$\sigma(\Delta)=\frac{4\pi^2\chi^2}{3\bar{v}}\frac{\mathcal{V}_0}{\omega^2|C_2-C_3|^{5/6}}\frac{1}{|\Delta|^{1/6}} , \tag{2.55}$$

in agreement with the behavior found by Gallagher and Holstein.[7]

III. NUMERICAL CALCULATIONS

In this section we indicate the results obtained through numerical calculations of the LICET transition and compare them with the approximate solutions obtained in Sec. II. All these results refer to the case of collisions between europium atoms and strontium atoms, whose energy-level scheme, shown in Fig. 2, is similar to the one shown in Fig. 1.

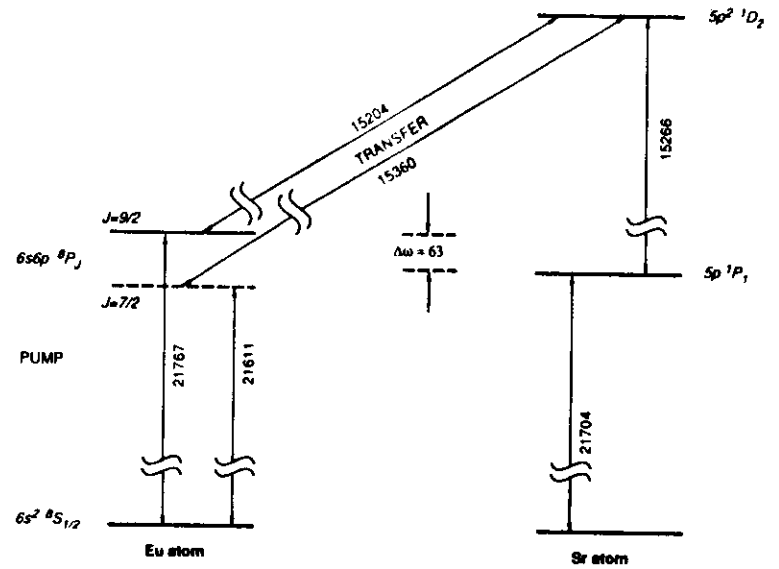

FIG. 2. Energy-level diagram for the LICET reaction with europium and strontium atoms. The Eu ($6s6p\ ^8P_J$) state is prepared by excitation (at 21 767 cm^{-1} for $J=9/2$ or at 21 611 cm^{-1} for $J=7/2$) from the ground state, using a dye laser (pump). The transition frequencies in the figure are expressed in cm^{-1}. The frequency defect between the Eu-Sr states $|1\rangle$ and $|2\rangle$ is $\Delta\omega=63\ cm^{-1}$.

The europium atoms are prepared initially in the $J=9/2$ state, while the strontium atoms are in their ground ($J=0$) state. During the collision, the excitation energy of Eu atoms is transferred to the Sr atoms, which at the end of the collision are in the $J=2$ state, while the Eu atoms are left in their ground state.

The compound atomic states for this system are so defined: state 1, Eu atom in the ground state, Sr atom in the $J=1$ state; state 2, Eu atom in the $J=9/2$ state, Sr atom in the ground state (initial state of the transition); state 3, Eu atom in the ground state, Sr atom in the excited state $J=2$ (final state of the transition).

This configuration and the energies of the atomic levels involved in the transition are shown in Fig. 2. The laser field is tuned near resonance for the interatomic transition $Eu(J=9/2) \to Sr(J=2)$. The quasistatic wing for this LICET transition extends towards the red ($\Delta<0$) side of the resonance peak. The van der Waals level shifts for this configuration are negligibly small, in comparison with ω_z (ω_z), so that we expect to find the far-wing behavior given in Eq. (2.38). The collisional interaction energy (dipole-dipole interaction) has been assigned the value

$$\mathcal{V}_0=2.17\times10^{-35}\ erg\ cm^3 , \tag{3.1}$$

which is consistent with the value used in Ref. 14.

The frequency difference between state 1 and state 2 is $63\ cm^{-1}$. With these values, the interatomic separation at which $\mathcal{V}_0/R^3$ equals the frequency difference is $R_z=12.2$ Å. When the frequency detuning $|\Delta|$ of the laser field is of order of ω, transitions occur when the atoms are near the interatomic distance R_z at which the phase is stationary. In this region of the spectrum, the cross section should therefore follow the law given by Eq. (2.38).

We have numerically integrated the equations (2.3a)-(2.3c) starting from the initial conditions (2.6a)-(2.6c) with assigned values of b and v. The integration time was from -60 to $+60$ psec. At the end of the integration $|a_3|^2$ would give the transition probability.

In Fig. 3 the evolution with time of the intermediate state 1 is reported. The impact parameter b is 12 Å, the relative speed v is 5×10^4 cm/sec, and the frequency detuning Δ is $-26.6\ cm^{-1}$ (quasistatic wing). The dotted curve displays $|a_1(t)|^2$ versus time, as evaluated from Eq. (2.24), while the solid line represents the behavior of $|a_1|^2$ evaluated by the numerical integration. This graph shows that the instantaneous diagonalization used in deriving (2.24) is a very good approximation for the evaluation of the population of state 1 during the collisional process. As expected, the population grows to large values (of the same order of magnitude as the population of state 2) at finite times, and then goes back to very low values (zero in the approximate model) when t

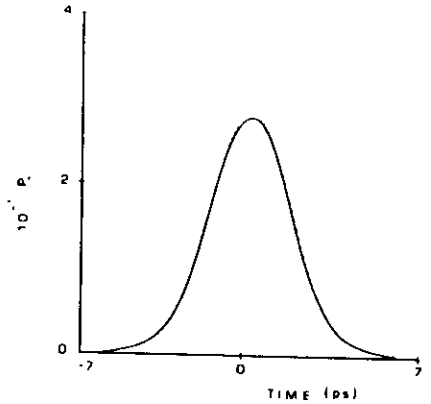

FIG. 3. Behavior of the Eu-Sr intermediate state probability $P_1 = |a_1(t)|^2$ vs time. The dotted line is calculated from Eq. (2.24). The solid line is the behavior of P evaluated by numerical integration. The values of the parameters are $b = 1.2$ nm and $\Delta = -26.6\ \mathrm{cm}^{-1}$. In all calculations we have taken the field intensity equal to 0.05 MW/cm^2 and the relative speed equal to 5×10^4 cm/sec.

goes to infinity. The difference between the two curves is due to the fact that we have neglected both transitions between the dressed states b_1 and b_2 [term $\dot{\theta}$ in Eq. (2.21)] and transitions to the final level a_3.

In Fig. 4 we have reported the corresponding graphs for the population of the final state (state 3) versus time during the same collisional event. Here again, the dotted

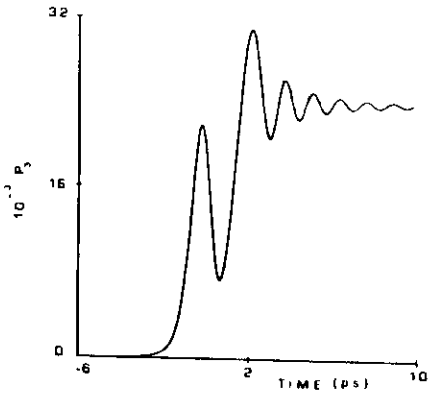

FIG. 4. Behavior of the Eu-Sr final state probability $P_3 = |a_3(\infty)|^2$ vs time. The dotted line is calculated from Eq. (2.25). The solid line is the behavior of P_3 as given by the numerical integration. The values of the parameters are the same as in Fig. 3.

curve is evaluated from the approximate solution [Eq. (2.25)], while the solid line represents the time evolution of $|a_3|^2$ as given by the numerical integration. We have compared the approximate model and the numerical integration for several other values of the impact parameter and the relative speed, and we have found that they were in good agreement, the difference being less than a few percent in most cases.

In Figs. 5 and 6 we show the graphs of $|a_3(+\infty)|^2$ versus the impact parameter b at fixed v. The dotted line is evaluated from Eq. (2.25), while the solid line represents the values found by numerical integration. Here again, the validity of the approximation of instantaneous diagonalization is apparent. In Fig. 5 the transition probability is evaluated at resonance, and in Fig. 6 at $\Delta = -26.6\ \mathrm{cm}^{-1}$.

Both graphs display the oscillatory behavior of $|a_3(+\infty)|^2$ when b is made to vary. Off resonance, this is explained as an interference effect between the two points at which frequency matching occurs. At resonance, the oscillations are also present, bu: only at low values of the impact parameter, for which the amplitude of the final level goes through several nodes because of the exponential factor in Eq. (2.25). At resonance, however, the relevant contributions to the cross section come from collisions occurring at large values of b, in which the levels involved in the transition are practically unperturbed at all times, and their frequency difference matches the laser frequency. In the latter case, the transition does not occur at (or around) some interatomic separation, rather there is a continuous flow of population from the initial level to the final level during the time of the collisional interaction.

The solid curve in Fig. 7 represents the same graph as those shown in Fig. 6, but evaluated by using Eq. (2.30), i.e., the method of the stationary phase. For comparison, the dotted line in Fig. 7 shows the results from numerical integration.

As expected, the method of stationary phase provides an accurate evaluation of the transition probability only when the impact parameter is smaller than the interatomic separation R_s where stationary phase occurs. When b equals this interatomic separation, the probability $|a_3(+\infty)|^2$, evaluated by using the stationary phase, diverges. The full spectrum of LICET transition has been numerically evaluated for the europium-strontium colliding partners. We have used a Monte Carlo simulation in which the transition probabilities $|a_3(+\infty)|^2$ were found by means of Eq. (2.25) [or Eq. (2.30) when applicable] for various values of the impact parameter b and the relative speed v, chosen at random from their own distributions. These calculations were made with the purpose of checking whether the two-slope behavior, as given by Eq. (2.38) remains valid when the interference between the points of stationary phase and the average over relative speed are taken into account.

Figure 8 shows the results for the Monte Carlo simulation of the spectrum. The laser detuning is in the range from 0 to $-53.1\ \mathrm{cm}^{-1}$, extending towards the red wing of the spectrum where quasistatic transitions take place. The field intensity was chosen 0.05 MW/cm^2, i.e., well

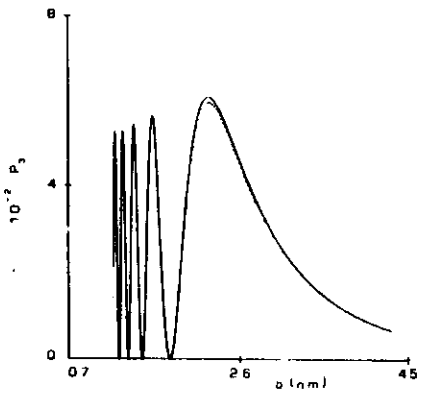

FIG. 5. Graphical comparison of the transition probability $P_3 = |a_3(t=\infty)|^2$ vs impact parameter b at a fixed value of v for the Eu-Sr LICET reaction. The dotted line is calculated from Eq. (2.25) while the solid line is found by numerical integration. The laser frequency is tuned at resonance with the LICET transition frequency $\omega_3 - \omega_2$. The graph displays rapid oscillations for low values of b and a smoother behavior for larger values of b. The boundary between these two regions is roughly at the Weisskopf radius.

within the linear regime. Since in this range the cross section is expected to increase linearly with the field intensity, we have plotted the values for σ/I instead of those for σ. At resonance, the cross section was found to be 680 Å^2/(MW/cm^2), a value in good agreement with previous estimates for the Eu-Sr colliding partners.[13]

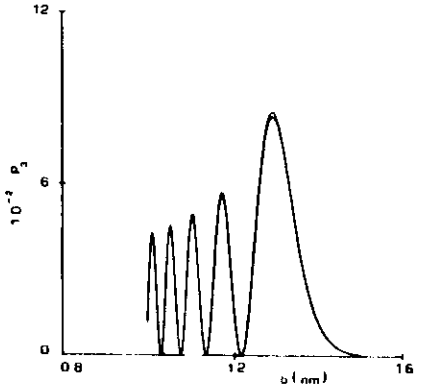

FIG. 6. Graphical comparison of the transition probability $P_3 = |a_3(t=\infty)|^2$ vs the impact parameter b at a fixed value of v for the Eu-Sr LICET reaction. The dotted line is calculated from Eq. (2.25) while the solid line is found by numerical integration. The detuning is $\Delta = \Omega - \hbar^{-1}(E_3 - E_2) = -26.6\ \mathrm{cm}^{-1}$.

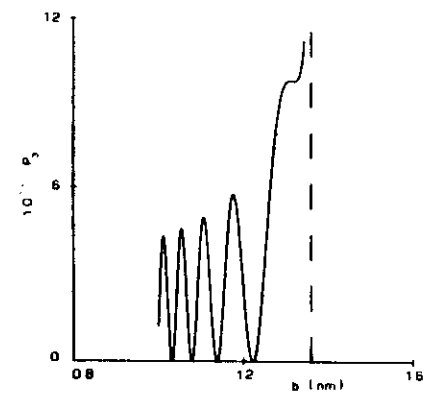

FIG. 7. Graphical comparison of the transition probability $P_3 = |a_3(t=\infty)|^2$ vs the impact parameter b at a fixed value of v for the Eu-Sr LICET reaction. The detuning of the laser frequency from the LICET transition frequency $\hbar^{-1}(E_3 - E_2)$ is $\Delta = -26.6\ \mathrm{cm}^{-1}$. The dotted line is calculated from Eq. (2.25); the solid line results from the application of the method of stationary phase. As expected, the stationary phase result diverges when b equals the interatomic separation R_s.

The values of the cross section in the red wing, evaluated from the Monte Carlo simulation, was found to differ by 15% from the values obtained by means of Eq. (2.38), the latter being the smaller. This discrepancy is explained by the fact that in deriving Eq. (2.38) we have replaced the phase factor and the relative speed by their averages.

However, the slopes of the line shape in the quasistatic wing, evaluated from the numerical simulation and from the analytic expression, are in good agreement. We show a logarithmic plot of both in Fig. 9. The solid line is from

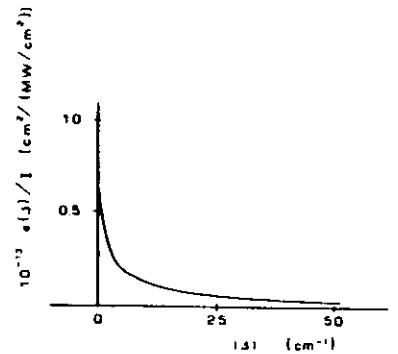

FIG. 8. Graph of the LICET spectrum from Monte Carlo simulation of the Eu-Sr LICET reaction. Detuning ranges from 0 to $-53.1\ \mathrm{cm}^{-1}$.

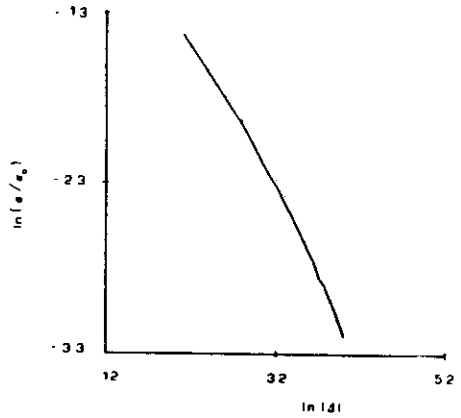

FIG. 9. Log-log plots of the LICET spectrum in the far wing for the Eu-Sr LICET reaction. The dotted line, obtained from Eq. (2.38), is the same as in Fig. 7. The solid line is from Monte Carlo simulation. The detuning is in the range from -8 to -53.1 cm^{-1}. The two curves were arbitrarily assumed to be equal at $\Delta=-8$ cm^{-1}.

the Monte Carlo simulation and the dotted line from Eq. (2.38). The two curves were arbitrarily taken to be equal at $\Delta=-8$ cm^{-1}. We see that the local slope in the Monte Carlo simulation increases when $|\Delta|$ increases, and its values are quite consistent with those derived from Eq. (2.38).

These calculations show that the approximations used in this work give quite accurate results. Both instantaneous diagonalization and stationary phase methods were checked for the case of europium and strontium colliding partners. We found that in most cases, the deviations of the approximate results from the values obtained through numerical integration were small. The only case in which the approximations used to derive Eq. (2.38) lead to values that deviate considerably from the exact results is when the trajectory of the colliding partners happens to be close to the tangent to the sphere of radius R_s, where R_s is the distance at which stationary phase occurs. This is shown clearly by the graphs of Fig. 7. However, the singularity of the cross section disappears when integrated over the distributions of the impact parameter. Moreover, as can be seen from the same figure, the area of the curve $|a_3|^2$ evaluated from the stationary phase method and lying above the exact $|a_3|^2$ curve is roughly compensated by the area of the tail of the exact curve extending beyond R_s.

IV. DISCUSSION AND CONCLUSION

In this paper we have extended and described in greater detail the three-state LICET model presented in Refs. 10 and 11. This model replaces the two-level model in all cases in which an intermediate level lies very close to either the initial or final level of the transition, with a frequency mismatch of the same order as the laser detuning at which the cross section is being measured. Since this is a situation which is often realized experimentally, the cross sections shown in this paper should be used for predicting the behavior of the quasistatic wing for large detunings.

When the van der Waals shifts are included in the treatment, we have shown that the LICET line shape may follow different laws depending on the relative strength of the collisional interaction with respect to the level shifts. For a dipole-dipole interaction, we have discussed several possible cases that arise in different situations. For a dipole-quadrupole interaction, we have not presented any detailed result, but the cross section can be easily evaluated from the general formulas in Sec. II, according to the specific case under investigation.

This model has also been shown to lead to the known results (a $-1/2$ power law for the dipole-dipole interaction and a $-1/6$ power law for the dipole-quadrupole interaction) in the limit case when the intermediate level behaves very much as a true virtual level, i.e., its frequency mismatch is large when compared to the laser detunings at which the cross section is measured. This model has been applied to the derivation of the cross section for a LICET process in an energy configuration scheme such as the one shown in Fig. 1, but other configuration schemes may be worked out as well. A different energy-level scheme, valid for the LICET process with strontium and lithium atoms, is treated in Appendix B. The cross section in the far wing for this process is the same as the one found for the scheme in Fig. 1. This model should also apply in other cases of collisionally aided energy transfer, when there are energy levels, lying nearby the initial or the final level, that are adiabatically populated during the collisional interaction. All the approximations used in the derivation of the cross section [Eqs. (2.38), (2.41), and (2.44)] have been checked by numerical computations of the differential equations for the level amplitudes. The Monte Carlo simulation of the LICET spectrum displays the variable slope feature of the far wing, as predicted by Equation (2.38).

In Ref. 11 it has been shown that the far-wing behavior predicted by this model fits the experimental data found for Eu-Sr,[15] Na-Ca,[16] and Sr-Li.[12] In particular, in the experiment on Sr-Li colliding partners, the frequency mismatch is 21 cm^{-1}, while the far wing has been measured up to 50 cm^{-1}. Thus one would expect a substantial change in the local slope of the spectrum in this range of frequency detunings. It has been found that the local slope varies between -0.5 to -2 in the range 5–50 cm^{-1}, which are the extreme values predicted by this model in the two limits $\Delta \ll \omega$ and $\Delta \gg \omega$. In a recent experiment[17] the far wing for the Eu-Sr case has been measured up to 55 cm^{-1}. In this experiment the average slope of the wing was found equal to -0.7 in the range 6–30 cm^{-1}, and equal to -1.1 in the range 30–53 cm^{-1}, in good agreement with the predictions of this model.

A few questions remain unanswered, for instance, the role of the magnetic sublevels in the transition and the effects of the transfer of energy from the translational degrees of freedom to the electronic excitation (or vice versa), which occur at large frequency detunings. However, the accuracy of the existing experimental data does not allow one to assess whether these effects are important or not. Experimental evidence exists only for the variation of the local slope in far wing of the LICET spectrum, and the present model seems to agree fairly well with the experimental data reported to date.

ACKNOWLEDGMENTS

The authors would like to thank Professor P. E. Toschek for providing us with his results (Ref. 12) prior to publication. The work of P. R. B. is supported by the U. S. Office of Naval Research.

APPENDIX A

The integral in Eq. (2.25) gives the probability amplitude of the final level of the LICET process. When the laser frequency is not resonant with the transition, the exponential factor in the integrand function oscillates for almost all times, except those (if they exist) in which the exponent passes through a maximum or a minimum, i.e., its derivative, which represents the instantaneous frequency mismatch, is zero. The method of stationary phase makes use of this fact to provide an approximate evaluation of the integral.

We derive now the conditions that must be satisfied for this approximation to be valid. For the sake of clarity, we derive these conditions in the simple case where $S_1=S_2=S_3=0$ and the interaction potential is a dipole-dipole potential.

The first, obvious, condition is that the exponent in the integrand function must be stationary at some points. But this condition is not sufficient. We must also require that the time intervals, centered around the points of stationarity where transition occurs, are much shorter than the collision time T_c, over which integration in Eq. (2.25) is carried out.

Transitions can occur only when the instantaneous frequency mismatch is compensated by the rate of change of the interaction potential, i.e., when it does not exceed ν, with

$$\nu \equiv \left| \frac{\dot{V}_{12}}{V_{12}} \right| = \frac{6v^2 t_s}{R_s^2} \ . \tag{A1}$$

Around the point of stationarity we can assume that the instantaneous energy of the dressed quasimolecular level b_2 varies linearly with time. Thus

$$\lambda_2 \approx \left| \frac{\partial \lambda_2}{\partial t} \right|_s (t-t_s) = \nu \frac{\mathcal{V}_0^2}{R_s^6} \frac{1}{(\omega^2+4V_{12}^2)^{1/2}} (t-t_s) \ , \tag{A2}$$

where s indicates that the rhs of (A2) is evaluated at the point of stationarity, where the frequency mismatch is zero. The time interval in which transitions may occur can then be estimated by equating (A1) to (A2). We find that this time interval is given by

$$\tau = t - t_s \approx \frac{R_s^6(\omega^2+4V_{12}^2)^{1/2}}{\mathcal{V}_0^2} \ . \tag{A3}$$

At the point of stationarity we also have

$$\frac{\mathcal{V}_0^2}{R_s^6} = |\Delta|(\omega+|\Delta|) \ , \tag{A4}$$

$$(\omega^2+4V_{12}^2)^{1/2} = \omega+2|\Delta| \ . \tag{A5}$$

Substituting (A4) and (A5) in Eq. (A3) and requiring that τ must be much smaller than T_c, we find the second condition for the validity of the method of stationary phase:

$$\frac{1}{|\Delta|} + \frac{1}{\omega+|\Delta|} \ll T_c \approx b/v \ . \tag{A6}$$

This condition requires that the detuning must be large compared to T_c^{-1}. Typical values for T_c are in the range of 10^{-11} sec. Then $|\Delta|$ must be larger than a few cm^{-1} for our approximations to be valid.

APPENDIX B

In this appendix we derive the relevant formulas for the cross section in a LICET process occurring between atoms with a different energy-level scheme. As shown below, Eq. (B30), the cross section in the wing has the same form as in Eq. (2.38), although the sign of the detuning Δ is now reversed. The calculations in this appendix apply to the case of strontium-lithium colliding partners, which have been used in another LICET experiment.[12] The energy levels of these atoms, involved in the transition, are shown in Fig. 10.

We perform these calculations in their simplest form, namely, we ignore all couplings except those that drive the LICET transition. Shifts due to virtual processes, namely the Stark and the van der Waals shifts, are neglected. The Sr atoms are prepared initially in the excited state α^* ($5s5p\ ^1P_1$), while the Li atoms are in their ground state β ($2s\ ^2S_{1/2}$). During the collision, a photon is absorbed by the system, and energy transfer occurs from state (α^*,β) to state (α,β^{**}). The frequency mismatch between these two states is 21 cm^{-1}. We label the compound atomic states as

$$|1\rangle = |\alpha^*\rangle|\beta\rangle \ , \tag{B1}$$

$$|2\rangle = |\alpha\rangle|\beta^{**}\rangle \ , \tag{B2}$$

$$|3\rangle = |\alpha^*\rangle|\beta^*\rangle \tag{B3}$$

(see Fig. 10). The equations for the Schrödinger amplitudes now read

$$i\dot{c}_1 = \omega_1 c_1 + \chi e^{i\Omega t} c_3 \ , \tag{B4}$$

$$i\dot{c}_2 = \omega_2 c_2 + V c_3 \ , \tag{B5}$$

$$i\dot{c}_3 = \omega_3 c_3 + V c_2 + \chi e^{-i\Omega t} c_1 \ , \tag{B6}$$

where $\hbar\omega_j$ are the energies of the levels, χ is the atom-field coupling, and the collisional (dipole-dipole) interaction V is given by

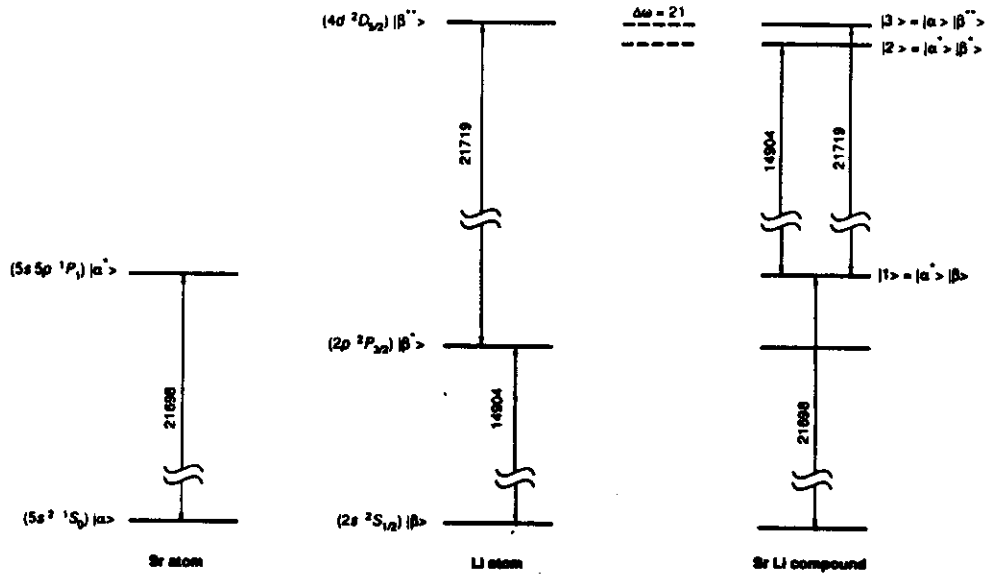

FIG. 10. Energy-level diagram for the LICET reaction between strontium atoms and lithium atoms. The Sr $(5s5p\ ^1P_1)$ state is prepared by excitation at 21 698 cm^{-1} from the ground state using a dye laser. The LICET transition occurs at 14 525 cm^{-1}. The frequency defect between the final state $|3\rangle$ and the intermediate compound state $|2\rangle$ is $\Delta\omega = 21\ cm^{-1}$.

$$V = \frac{\mathcal{V}_0}{R^3} . \tag{B7}$$

In first-order perturbation theory we ignore the term χ in the Eq. (B4). Thus the population of the initial level remains unperturbed,

$$i\dot{c}_1 \simeq \omega_1 c_1 \Longrightarrow c_1 \simeq e^{-i\omega_1 t} . \tag{B8}$$

Substituting this expression for c_1 in Eqs. (B5) and (B6), we get the following system:

$$i\dot{c}_2 = \omega_2 c_2 + V c_3 , \tag{B9}$$

$$i\dot{c}_3 = \omega_3 c_3 + V c_2 + \chi e^{-i(\Omega+\omega_1)t} . \tag{B10}$$

For convenience, we define the reference energy in (B9) and (B10) as the average

$$\nu = \frac{\omega_2 + \omega_3}{2} \tag{B11}$$

and the slowly varying amplitudes

$$a_2 = c_2 e^{-i\nu t} , \tag{B12}$$

$$a_3 = c_3 e^{-i\nu t} , \tag{B13}$$

which satisfy the system

$$i\frac{d}{dt}\begin{vmatrix} a_2 \\ a_3 \end{vmatrix} = \mathcal{A}\begin{vmatrix} a_2 \\ a_3 \end{vmatrix} + \begin{vmatrix} 0 \\ F(t) \end{vmatrix} , \tag{B14}$$

where the source term $F(t)$ is

$$F(t) = \chi e^{-i(\Omega+\omega_1-\nu)t} \tag{B15}$$

and the matrix $\mathcal{A}$ is

$$\mathcal{A} = \begin{vmatrix} \omega & V \\ V & -\omega \end{vmatrix}, \quad \omega = \frac{\omega_2 - \omega_3}{2} . \tag{B16}$$

We pass now to a dressed atom picture in which the two states a_2 and a_3 are dressed by their collisional interaction. We define the vector b as

$$\mathbf{b} = \begin{vmatrix} b_f \\ b_x \end{vmatrix} \equiv \mathcal{I}\begin{vmatrix} a_2 \\ a_3 \end{vmatrix} , \tag{B17}$$

$\mathcal{I}$ being an orthogonal matrix of the form

$$\mathcal{I} = \begin{vmatrix} \cos\theta & -\sin\theta \\ \sin\theta & \cos\theta \end{vmatrix} , \tag{B18}$$

which instantaneously diagonalizes the matrix $\mathcal{A}$. Here the vector b follows a equation of the type (neglecting transitions between b_f and b_x)

$$i\dot{\mathbf{b}} = \underline{D}\mathbf{b} + \mathcal{I}\begin{vmatrix} 0 \\ F(t) \end{vmatrix} , \tag{B19}$$

where $\underline{D}$ is the diagonal matrix whose elements λ_f and λ_x are the solution of the equation

$$\det|\mathcal{A} - \lambda\underline{I}| = 0 . \tag{B20}$$

Both components of the vector b, in contrast with the previous case, are now different from zero. We find

$$b_f = i\exp\left[-i\int_{-\infty}^{t}\lambda_f dt'\right] \times \int_{-\infty}^{t} dt' \sin(\theta) F(t') \exp\left[i\int_{-\infty}^{t'}\lambda_f dt''\right] , \tag{B21}$$

$$b_x = -i\exp\left[-i\int_{-\infty}^{t}\lambda_x dt'\right] \times \int_{-\infty}^{t} dt' \cos(\theta) F(t') \exp\left[i\int_{-\infty}^{t'}\lambda_x dt''\right] \tag{B22}$$

and, inverting (B17), we obtain

$$a_2(t) = \cos(\theta) b_f + \sin(\theta) b_x . \tag{B23}$$

It is seen immediately that $\sin(\theta) \to 0$ when $t \to \infty$. Thus the final level amplitude is given, at $t = +\infty$, by

$$a_2(+\infty) = b_f(+\infty) = i\exp\left[-i\int_{-\infty}^{+\infty}\lambda_f dt'\right] \times \int_{-\infty}^{+\infty} dt' \sin(\theta) F(t') \exp\left[i\int_{-\infty}^{t'}\lambda_f dt''\right] . \tag{B24}$$

The eigenvalue λ_f that appears in (B24) is given by

$$\lambda_f = (\omega^2 + V^2)^{1/2} . \tag{B25}$$

We can still apply the method of the stationary phase to find

$$-\Omega - \omega_1 + \nu + \lambda_f = 0 \quad \text{at } R = R_s , \tag{B26}$$

which gives

$$R_s = \left|\frac{\mathcal{V}_0}{\Delta(\omega_2 - \omega_3 + \Delta)}\right|^{1/6} . \tag{B27}$$

The value of $\sin(\theta_s)$ at the points of stationary phase now is

$$\sin(\theta_s) = \frac{1}{\sqrt{2}}\left|\frac{\Delta}{\omega + \Delta}\right|^{1/2} , \tag{B28}$$

while the second derivative of the phase gets the value, at the same points,

$$|\ddot{\phi}_s| = \frac{1}{\omega + \Delta}\frac{3\mathcal{V}_0^2 v}{R_s^7}\left|1 - \frac{b^2}{R_s^2}\right|^{1/2} . \tag{B29}$$

Using (B27)–(B29) we obtain, for the cross section in the far wing, with the same approximations used to derive (2.38),

$$\sigma(\Delta) = \frac{4\pi^2\chi^2}{3\bar{v}}\frac{\mathcal{V}_0}{\Delta^{1/2}(\omega_2 - \omega_3 + \Delta)^{3/2}} , \quad \Delta > 0 , \tag{B30}$$

which has the same form as Eq. (2.38). Notice that, in the Sr-Li case, the intermediate level lies just below the final level, so that the stationary phase occurs in the blue ($\Delta > 0$) wing of the LICET line shape.

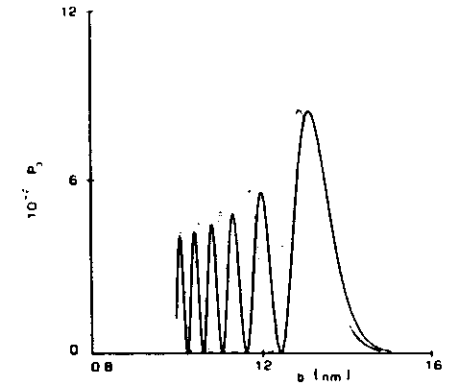

FIG. 11. Graphical comparison of the probability transition $P_3 = |a_3(t=\infty)|^2$ vs the impact parameter b for the Eu-Sr LICET reaction. The dotted curve is found by integrating numerically the three-level system with the detuning $\Delta = -26\ cm^{-1}$. The solid line is obtained by integration of a four-level system (Eu $J = 7/2$ state is included in the dynamic evolution of the system). There is a slight variation of the interatomic separation at which the points of stationary phase occur.

APPENDIX C

In the europium-strontium experiment the initial state in which europium atoms are prepared is either $^8P_{9/2}$ or $^8P_{7/2}$. The energy separation between these two states is 153 cm^{-1}, and, with respect to the $^1P_1$ $(J=1)$ state of strontium, the former lies 63 cm^{-1} above, and the latter 90 cm^{-1} below. The question arises as to whether or not the $P_{7/2}$ state of Eu has any effect on the LICET cross section for atoms initially prepared in the $J = 9/2$ state. Since the $^1P_1$ state of Sr is coupled to both states of Eu by a dipole-dipole interaction, one might expect that some population passes from the initial state of Eu to the other state of Eu during the collision. This fact would in turn decrease the adiabatic population of the $^1P_1$ state of Sr at small impact parameters, thereby decreasing the population transferred to the final state of Sr.

In this case one has to deal with a four-level problem, and the method of stationary phase used in Sec. II cannot be applied in a simple form. We have therefore numerically evaluated the final-level population after a single collision for several values of the impact parameter. The results are shown in Fig. 11 for the case of a frequency detuning equal to $-25\ cm^{-1}$ and Eu atoms initially prepared in the $J = 9/2$ state. The dotted line represents the $|a_3|^2$ versus b curve found by integrating numerically the three-level system, and the solid line is the graph for the four-level system.

We note that the main effect brought into the process by the presence of both europium states is a variation of the interatomic separation at which stationary phase occurs, which is roughly indicated by the position of the

ast peak in the $|a_3|^2$ versus b graph. This is primarily lue to the van der Waals shift induced on the $J=1$ state of Sr by the $J=7/2$ state of Eu.

There is also a small reduction in the final-level popula- ion, which is due to the fact that the extra level gets ome population during the collisional interaction (at $= +\infty$, however, there is no population left in this lev- l). However, this effect is very small and does not affect the transition cross section in the far wing. The peak at resonance is completely unaffected by the presence of the extra Eu level, as one would expect from the discussion in Sec. II: At resonance the main contributions to the tran- sition come from collisions occurring at large impact pa- rameters, in which the $J=1$ state of Sr and the extra level of Eu are not populated even during the collisional in- teraction.

S. I. Yakovlenko, Sov. J. Quant. Elec. **8**, 151 (1978).
M. G. Payne, V. E. Anderson, and J. E. Turner, Phys. Rev. A **20**, 1032 (1979).
P. R. Berman and E. J. Robinson, in *Photon Assisted Collisions and Related Topics*, edited by N. K. Rahman and C. Guidotti (Harwood, Chur, 1982), pp. 15–33.
S. E. Harris and D. B. Lidow, Phys. Rev. Lett. **33**, 674 (1974).
R. W. Falcone, W. R. Green, J. C. White, J. F. Young, and S. E. Harris, Phys. Rev. A **15**, 1333 (1977).
Ph. Cahuzach and P. E. Toschek, Phys. Rev. Lett. **40**, 1087 (1978).
A. Gallagher and T. Holstein, Phys. Rev. A **16**, 2413 (1977).
M. G. Payne and M. H. Nayfeh, Phys. Rev. A **13**, 595 (1976).
P. R. Berman, Phys. Rev. A **22**, 1838 (1980); **22**, 1848 (1980).
[9]A. Bambini and P. R. Berman, in *Workshop on Photons and Continuum States of Atoms and Molecules*, edited by N. K. Rahman, C. Guidotti, and M. Allegrini (Springer-Verlag, Berlin, 1987), pp. 220–226.
[11]A. Bambini and P. R. Berman, Phys. Rev. A **35**, 3753 (1987).
[12]F. Dorsch, Diploma thesis, University of Hamburg, 1986; F. Dorsch, S. Geltman, and P. E. Toschek, Phys. Rev. A **37**, 2441 (1988).
[13]A. Bambini and A. Stefanel, in *Collisions and Half Collisions with Lasers*, edited by N. K. Rahman and C. Guidotti (Harwood, Chur, 1984).
[14]K. Niemax, Phys. Rev. Lett. **55**, 56 (1985).
[15]C. Brechignac, Ph. Cahuzac, and P. E. Toschek, Phys. Rev. A **21**, 1969 (1980).
[16]A. Debarre, J. Phys. B **16**, 431 (1983).
[17]M. Matera, M. Mazzoni, R. Buffa, S. Cavalieri, and E. Arimondo, in *Workshop on Photons and Continuum States of Atoms and Molecules*, edited by N. K. Rahman, C. Guidotti, and M. Allegrini (Springer-Verlag, Berlin 1987), pp. 227–232; Phys. Rev. A **36**, 1471 (1987).